

The kinetic Hamiltonian with position-dependent mass

R. M. Lima¹ and H. R. Christiansen^{1,2*}

IFCE - Instituto Federal de Educação, Ciência e Tecnologia do Ceará,
CEP 62042-030 - Sobral¹, and CEP 61940-750 - Maranguape², Ceará, Brazil

Abstract

In the present paper we examine in a systematic way the most relevant orderings of *pure kinetic Hamiltonians* for five different position-dependent mass (PDM) profiles: soliton-like, reciprocal quadratic and biquadratic, exponential and parabolic. As a result of the non-commutativity between momentum and position operators, a diversity of effective potentials is generated. We analyse the whole set and find unexpected coincidences as well as discrepancies among them. We obtain analytically the full-spectrum of energies and solutions in the twenty-five cases considered. It is shown how the simple ordinary constant-mass solutions are transformed into a variety of complex combinations of transcendental functions and arguments. We find that particles with a non-uniform mass density can present discrete energy spectra as well as continuous ones which can be bounded or not. These results are consistent with the fact that although the external potential is zero, PDM eigenfunctions are not actual free states but a sort of effective waves in a solid-state sample. This is precisely the origin of the position-dependent mass. In all the events we obtain exact complete spectral expressions. Our methodological procedure thus puts a wide diversity of Hamiltonian seeds on an equal footing in order to be compared. This allows choosing the better arrangement to model a specific solid or heterostructure once the spectrum of a given material is experimentally available. Finally, we perform a one-dimensional model calculation of a double heterostructure with a parabolic PDM particle in the interface region. Our study is also indicated for applications inside material structures with the addition of external potentials.

Keywords: quantum mechanics; position-dependent mass; analytical spectrum; quantum heterostructures.

Published in *Physica E: Low dimensional Systems and Nanostructures* 150 (2023) 115688.

*Corresponding author. Electronic address: hugo.christiansen@ifce.edu.br

1 Introduction

Quantum Mechanics of particles with non-uniform masses has always been matter of concern for the Hamiltonian's dependence on the ordering of the dynamical variables. This problem was born in the realm of solid-state physics [1–5] and soon became of interest from a rather more fundamental point of view regarding basic symmetries [6–10].

Position-dependent mass (PDM) models have been under regular development since the sixties and continuously improved up to present days. Particularly, in the last decade modeling quantum systems with PDM particles has grown as a consequence of its wide area of applications [11–16]. Among them, this technique has been applied to the understanding of the electronic properties of semiconductor heterostructures, crystal-growth techniques [5, 17], quantum wells and quantum dots [18–28], helium clusters [29], graded crystals [30], quantum liquids [31], nanowire structures with size variations, impurities, dislocations, and geometry imperfections [32–35], as well as in superconductors investigations [4, 5, 7, 17, 30, 36–40].

Concomitantly, the dynamics of quantum systems has been extensively studied in connection with all kind of problems, from low to high energy physics. Mathematically, the problem consists in dealing with a Schrodinger equation, which, for stationary systems, results in an eigenvalue problem in a Hilbert space [41].

The number of exactly solvable potentials is relatively limited in ordinary quantum mechanics but as soon as we switch the constant mass into a position-dependent distribution the mathematical challenge grows dramatically. In order to treat analytically these problems, different methods have been used. We will apply point canonical transformations, which keep invariant the canonical form of the wave equation [11, 21, 22, 42, 43], but there exist alternative procedures like super-symmetric quantum mechanics [44–46], Lie algebras [47] and Weyl integral quantization [48, 49] (more refs. in [23, 50]), which have been also used in the last years.

For a non-uniform mass, $M \equiv M(\mathbf{r})$, the most general Hermitian kinetic Hamiltonians¹ is given by [7]

$$\hat{T}_{a,b}(\mathbf{r}) = \frac{1}{4} \left(M^a \hat{\mathbf{p}} M^{-1-a-b} \hat{\mathbf{p}} M^b + M^b \hat{\mathbf{p}} M^{-1-a-b} \hat{\mathbf{p}} M^a \right), \quad (1)$$

where $a, b \in \mathbb{R}$ are mass parameters and $\hat{\mathbf{p}} \equiv -i\hbar\nabla$.

Some particular cases of this expression are common in the literature and will be here studied and abbreviated by BDD (BenDaniel & Duke) [4] ($a = b = 0$), GW (Gora & Williams) [5, 17, 36, 55] ($a = -1, b = 0$), ZK (Zhu & Kroemer) [37] ($a = b = -1/2$), LK (Li & Kuhn) [55] ($a = 0, b = -1/2$) and MM (Mustafa & Mazharimousavi) [25] ($a = b = -1/4$) Hamiltonians (or orderings). In [7] the inherent ambiguity resulting from the mass parameters and the breaking of Galilean

¹ For a digression on non-Hermitian Hamiltonians see [51, 52]. It is also worth noting that the parity-time symmetry, although weaker than hermiticity, has been proven to allow unitary time-evolution in some cases; see [53] and [54].

invariance (except when considering the BDD ordering²) are also pointed out — however, it is worth noting that other authors [26, 45] came up with generalizations and even alternatives to the von Roos’ Hamiltonian shown to respect Galilean transformations —; furthermore, when abrupt heterojunctions (characterized by finite discontinuities in the position dependent mass) are considered [56] just $a = b$ orderings are viable, provided the continuity conditions (in one dimension) are imposed on $M^a\Psi(x)$ and $M^{-1-a}\Psi'(x)$. The manifest Galilean invariance and the vanishing of the ambiguous potential of kinetic origin (see below) seem to be the main reasons that made of BDD the most consensual kinetic Hamiltonian in the literature e.g. [21, 22, 42, 43]. Some experimental fits with BDD mass parameters can be also found in [39, 57]. Notwithstanding, the other orderings have been adopted with success in some systems [50], particularly when interfaces are not brusque. For example, in the case of exponential modeling of potential and mass within a material, the BDD ordering is the one to be discarded [58].

The plan of the present work is the following. In Section 2 we obtain a differential equation for a wave function involving only dimensionless quantities; in Subsection 2.1 we focus on the one-dimensional case and apply point canonical transformations in order to attain a Schrödinger equation for a new wave function in a space where the mass is constant. In Section 3 we analyze, assuming the absence of external potential, the following five mass profiles: the soliton-like and reciprocal biquadratic profiles (Subsection 3.1), the reciprocal quadratic profile (Subsection 3.2), the exponential profile (Subsection 3.3) and the parabolic profile (Subsection 3.4). In each case we obtain the effective potentials and the full spectrum of energy and exact analytical solutions. We also plot the probability densities associated with them. In Section 4 we solve the problem of a one-dimensional double heterostructure using a parabolic PDM particle inside the heterojunction among substances characterized by different mass carriers. Finally, in Section 5 we present our conclusions.

2 The dynamical equation for the wave function

We now rewrite the kinetic Hamiltonian above in order to make explicit the ambiguity sector,

$$\hat{T}_{a,b}(\mathbf{r}) = \frac{1}{2M}\hat{\mathbf{p}}^2 - \frac{1}{2M}\left(\frac{1}{M}\hat{\mathbf{p}}M\right) \cdot \hat{\mathbf{p}} + U_{a,b}(\mathbf{r}), \quad (2a)$$

where

$$U_{a,b}(\mathbf{r}) \equiv \frac{1}{2M}\left[\frac{a+b}{2}\hat{\mathbf{p}}\left(\frac{1}{M}\hat{\mathbf{p}}M\right) - \left(ab + \frac{a+b}{2}\right)\left(\frac{1}{M}\hat{\mathbf{p}}M\right)^2\right] \quad (2b)$$

²Indeed, in [9] BDD is deduced after Galilean invariance (similar results can be found in [8]).

behaves like a potential term of kinetic origin (it is noteworthy that, among the Hamiltonians here analyzed, the BDD ordering is the only one for which the ambiguity term is zero).

Should we add an external potential $V(\mathbf{r})$ to $\hat{T}_{a,b}(\mathbf{r})$ we would obtain the following differential equation for the wave function $\Psi(\mathbf{r})$ of the PDM particle

$$-\frac{\hbar^2}{2M}\nabla^2\Psi(\mathbf{r}) + \frac{\hbar^2}{2M}\frac{\nabla M}{M}\cdot\nabla\Psi(\mathbf{r}) + (U_{a,b}(\mathbf{r}) + V(\mathbf{r}))\Psi(\mathbf{r}) = E\Psi(\mathbf{r}),$$

$$U_{a,b}(\mathbf{r}) = -\frac{\hbar^2}{2M}\left[\frac{a+b}{2}\nabla\cdot\left(\frac{\nabla M}{M}\right) - \left(ab + \frac{a+b}{2}\right)\left(\frac{\nabla M}{M}\right)^2\right]. \quad (3)$$

This is a generalized Schrödinger equation and it is a very different differential equation from the ordinary constant-mass one.

We will transform the above equation by $\mathbf{r} \rightarrow \epsilon\mathbf{r}$, $\Psi(\mathbf{r}) \rightarrow \epsilon^{-D/2}\psi(\mathbf{r})$ and $M(\mathbf{r}) \rightarrow m_0m(\mathbf{r})$, where \mathbf{r} is, now, dimensionless; D is the number of spatial dimensions; ϵ and m_0 are positive constants with dimensions of length and mass, respectively; $\psi(\mathbf{r})$ and $m(\mathbf{r})$ are, respectively, the dimensionless and rescaled wave function and mass. The generalized Schrödinger equation becomes

$$-\frac{1}{m}\nabla^2\psi(\mathbf{r}) + \frac{1}{m}\frac{\nabla m}{m}\cdot\nabla\psi(\mathbf{r}) + (\tilde{U}_{a,b}(\mathbf{r}) + \tilde{V}(\mathbf{r}))\psi(\mathbf{r}) = \tilde{E}\psi(\mathbf{r}), \quad (4a)$$

where we write simply $m(\mathbf{r}) \equiv m$ and

$$\tilde{E} \equiv \frac{2\epsilon^2 m_0}{\hbar^2} E, \quad \tilde{V}(\mathbf{r}) \equiv \frac{2\epsilon^2 m_0}{\hbar^2} V(\epsilon\mathbf{r}) \quad \text{and}$$

$$\tilde{U}_{a,b}(\mathbf{r}) \equiv \frac{2\epsilon^2 m_0}{\hbar^2} U_{a,b}(\epsilon\mathbf{r}) = -\frac{1}{m}\left[\frac{a+b}{2}\nabla\cdot\left(\frac{\nabla m}{m}\right) - \left(ab + \frac{a+b}{2}\right)\left(\frac{\nabla m}{m}\right)^2\right] \quad (4b)$$

are the dimensionless and conveniently rescaled energy, external potential and ambiguity kinetic potential, respectively.

2.1 The Schrödinger equation for a new wave function in modified space-coordinates

For the one-dimensional case, when $\hat{p} \equiv -i\hbar\frac{d}{dx}$ and $m \equiv m(x)$, we will perform the change of variable

$$\frac{dz}{dx} = m^{1/2} \Leftrightarrow z(x) = \int^x \sqrt{m(x)} dx, \quad (5a)$$

mapping $\mathbb{R} \ni x \mapsto z \in \mathcal{D} \subset \mathbb{R}$, and define a function $\zeta(z)$ such that

$$\psi(x) = m^{1/4} \zeta(z(x)). \quad (5b)$$

Using this in eq. (4a) we obtain a Schrödinger equation for a particle with constant mass,

$$-\zeta''(z) + V_{a,b}(z)\zeta(z) = \tilde{E}\zeta(z), \quad (6a)$$

with a dimensionless effective potential given by

$$V_{a,b}(z) \equiv \tilde{V}(x(z)) + \frac{1}{m} \left[-\frac{1}{2} \left(a + b + \frac{1}{2} \right) \left(\frac{m'}{m} \right)' + \left(ab + \frac{a+b}{2} + \frac{3}{16} \right) \left(\frac{m'}{m} \right)^2 \right], \quad (6b)$$

where, for simplicity, we write $m' \equiv \left. \frac{dm}{dx} \right|_{x(z)}$ and $m \equiv m(x(z))$. Note that for the MM ordering, the effective potential stays simply $V_{a,b}(z) = \tilde{V}(x(z))$.

Since here we focus on the absence of external potentials, we will take $\tilde{V}(x) = 0$ everywhere. When the effective potentials $V_{a,b}(z)$ are symmetric around some point, we can write the general solution of eq. (6a), $\zeta_{a,b}(z)$, as a linear combination (LC) of particular symmetric and antisymmetric solutions around the same point. Once obtained the solutions that obey the boundary conditions, we use eqs. (5) to write the eigenfunctions in x space (our final goal).

It can be seen that the normalization condition for $\Psi(x)$ remains also valid for $\psi(x)$. On the other hand, by eqs. (5) it is easy to see that $|\psi(x)|^2 dx = |\zeta(z)|^2 dz$, which allows the interpretation of $\zeta(z)$ as a Schrödinger wave function in z space, normalized according to $\int_D |\zeta(z)|^2 dz = 1$, where $|\zeta(z)|^2$ is a probability density.

3 The mass profiles

In what follows, we present a variety of non-uniform continuous mass profiles that are found in the literature, some of which we cite along this paper. We study the differential equations resulting from considering such masses for the five most relevant Hamiltonian orderings. First we compute the effective potential in each case, and then we proceed to their analytical treatment. In every case we will obtain the exact full energy spectrum and the corresponding eigensolutions. We analyze the boundary conditions and display the probability densities of a representative number of states.

3.1 The soliton-like and reciprocal biquadratic profiles

Let us focus on two specific mass functions: the soliton-like profile³ [11–13],

$$M(x) = m_0 \operatorname{sech}^2 \left(\frac{x}{\epsilon} \right) \Leftrightarrow m(x) = \operatorname{sech}^2 x, \quad (7a)$$

³This profile can be particularly appropriate when hyperbolic potentials are considered. Also, it would possibly be the natural choice in the nonlinear Schrödinger equation with PDM where soliton solutions are present.

and the reciprocal biquadratic profile,

$$M(x) = m_0 \left[1 + \left(\frac{x}{\epsilon} \right)^2 \right]^{-2} \Leftrightarrow m(x) = (1 + x^2)^{-2} . \quad (7b)$$

As will become clear in what follows it will be convenient to treat these two different profiles together.

3.1.1 The effective potential

For the so-called soliton-like and reciprocal biquadratic mass distributions, eq. (5a) results in

$$\begin{cases} \operatorname{sech} x = \cos z & \text{(for the soliton-like profile)} \\ x = \tan z & \text{(for the reciprocal biquadratic profile)} \end{cases} , \quad (8)$$

both mapping $\mathbb{R} \ni x \mapsto z \in \left(-\frac{\pi}{2}, \frac{\pi}{2} \right)$. In this case, the effective potentials – eq. (6b) – parameterized with subindexes a and b are both given by

$$V_{a,b}(z) = \omega_{a,b} \tan^2 z + V_{a,b}^{(0)} , \quad (9a)$$

where

$$\omega_{a,b} \equiv 4ab + 2(a + b) + \frac{3}{4} \quad \text{and} \quad V_{a,b}^{(0)} \equiv V_{a,b}(0) = a + b + \frac{1}{2} \quad (9b)$$

for the soliton-like mass and

$$\omega_{a,b} \equiv 16ab + 6(a + b) + 2 \quad \text{and} \quad V_{a,b}^{(0)} \equiv V_{a,b}(0) = 2(a + b) + 1 \quad (9c)$$

for the reciprocal biquadratic mass (see Table 1).

Table 1: Values of $\omega_{a,b}$ and $V_{a,b}^{(0)}$ for the most relevant orderings and for each mass profile.

Orderings	soliton-like mass		Reciprocal biquadratic mass	
	$\omega_{a,b}$	$V_{a,b}^{(0)}$	$\omega_{a,b}$	$V_{a,b}^{(0)}$
BDD	3/4	1/2	2	1
GW	-5/4	-1/2	-4	-1
ZK	-1/4	-1/2	0	-1
LK	-1/4	0	-1	0
MM	0	0	0	0

The parameter $\omega_{a,b}$ determines the global behaviour of $V_{a,b}(z)$: when $\omega_{a,b} > 0$, $V_{a,b}(z)$ is an

infinite potential well; when $\omega_{a,b} < 0$, $V_{a,b}(z)$ is a bottomless barrier potential; finally, when $\omega_{a,b} = 0$, $V_{a,b}(z)$ is constant. The graphics of $V_{a,b}(z)$ can be seen in Fig. 1.

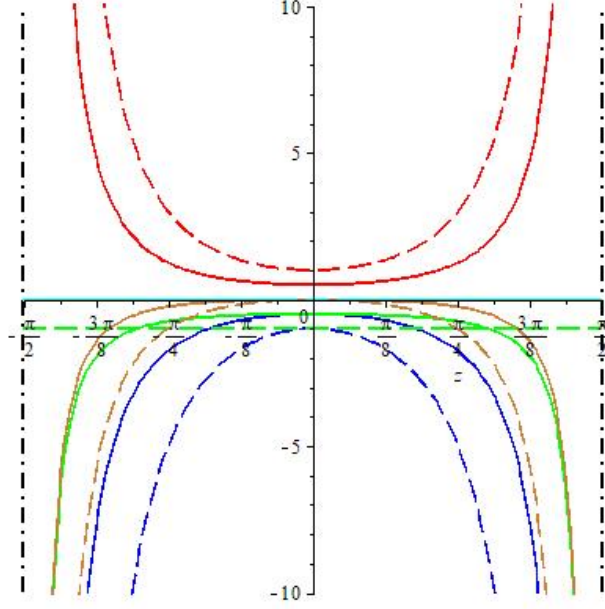


Figure 1: Shape of $V_{a,b}(z)$ for the soliton-like (solid lines) and reciprocal biquadratic (dashed lines) profiles and for the BDD, GW, ZK, LK and MM orderings (in red, blue, green, golden and cyan, respectively).

3.1.2 Solutions

Now we define the variable y by means of

$$y = \sin^2 z , \quad (10a)$$

which maps $\left(-\frac{\pi}{2}, \frac{\pi}{2}\right) \ni z \mapsto y \in [0, 1)$, and define a function $\xi(y)$ by

$$\zeta(z(y)) = y^\mu (1 - y)^\nu \xi(y) \quad , \quad \mu, \nu \in \mathbb{C} . \quad (10b)$$

Using this in eq. (6a) we obtain the differential equation

$$y(1 - y) \xi''(y) + \left[2\mu + \frac{1}{2} - (2\mu + 2\nu + 1) y \right] \xi'(y) + \left[\frac{\mu^2 - \frac{\mu}{2}}{y} + \frac{\nu^2 - \frac{\nu}{2} - \frac{\omega_{a,b}}{4}}{1 - y} + \frac{\mathcal{E}_{a,b} + \omega_{a,b}}{4} - (\mu + \nu)^2 \right] \xi(y) = 0 , \quad (11)$$

where $\mathcal{E}_{a,b} \equiv \tilde{E} - V_{a,b}^{(0)}$. $\mathcal{E}_{a,b}$ thus corresponds to the energy levels measured with respect to the value

of the effective potential at the origin.

Choosing μ and ν such that⁴

$$\mu^2 - \frac{\mu}{2} = 0 \Rightarrow \mu_{\pm} = \frac{1 \pm 1}{4} \quad \text{and} \quad \nu^2 - \frac{\nu}{2} - \frac{\omega_{a,b}}{4} = 0 \Rightarrow \nu_{a,b} = \frac{1}{4} \left(1 - \sqrt{1 + 4\omega_{a,b}} \right), \quad (12)$$

the above differential equation becomes

$$y(1-y)\xi''(y) + \left[2\mu_{\pm} + \frac{1}{2} - (2\mu_{\pm} + 2\nu_{a,b} + 1)y \right] \xi'(y) - \left[(\mu_{\pm} + \nu_{a,b})^2 - \frac{\mathcal{E}_{a,b} + \omega_{a,b}}{4} \right] \xi(y) = 0. \quad (13)$$

This is a hypergeometric Gauss equation,

$$\left\{ y(1-y) \frac{d^2}{dy^2} + [\gamma - (\alpha + \beta + 1)y] \frac{d}{dy} - \alpha\beta \right\} {}_2F_1(\alpha, \beta; \gamma; y) = 0, \quad (14)$$

where ${}_2F_1(\alpha, \beta; \gamma; y)$ is the hypergeometric Gauss function with parameters

$$\gamma_{\pm} \equiv 2\mu_{\pm} + \frac{1}{2} = 1 \pm \frac{1}{2}, \quad \alpha_{a,b}^{\pm} \equiv \mu_{\pm} + \nu_{a,b} + \frac{1}{2} \sqrt{\mathcal{E}_{a,b} + \omega_{a,b}} \quad \text{and} \quad \beta_{a,b}^{\pm} \equiv \mu_{\pm} + \nu_{a,b} - \frac{1}{2} \sqrt{\mathcal{E}_{a,b} + \omega_{a,b}}. \quad (15)$$

For each value of μ , one of the solutions around $y = 0$ is $\xi_{a,b}^{\pm}(y) = {}_2F_1(\alpha_{a,b}^{\pm}, \beta_{a,b}^{\pm}; \gamma_{\pm}; y)$. Since $\gamma_{\pm} \notin \mathbb{Z}$, a second independent solution is $\bar{\xi}_{a,b}^{\pm}(y) = y^{1-\gamma_{\pm}} {}_2F_1(\alpha_{a,b}^{\pm} + 1 - \gamma_{\pm}, \beta_{a,b}^{\pm} + 1 - \gamma_{\pm}; 2 - \gamma_{\pm}; y)$. By means of eqs. (10) we obtain the two independent solutions (even and odd) in z space:

$$\zeta_{a,b}^{\pm}(z) = (\sin z)^{2\mu_{\pm}} (\cos z)^{2\nu_{a,b}} {}_2F_1(\alpha_{a,b}^{\pm}, \beta_{a,b}^{\pm}; \gamma_{\pm}; \sin^2 z). \quad (16)$$

The solutions in x space are obtained using eqs. (5b), (8) and (16). For the soliton-like mass, one has

$$\begin{aligned} \psi_{a,b}^{\pm}(x) &= (\tanh x)^{2\mu_{\pm}} (\operatorname{sech} x)^{2\nu_{a,b} + \frac{1}{2}} {}_2F_1(\alpha_{a,b}^{\pm}, \beta_{a,b}^{\pm}; \gamma_{\pm}; \tanh^2 x) \\ &= (\tanh x)^{2\mu_{\pm}} (\operatorname{sech} x)^{2\nu_{a,b} + \frac{1}{2}} \times \\ &\quad \times {}_2F_1\left(\mu_{\pm} + \nu_{a,b} + \frac{1}{2} \sqrt{\mathcal{E}_{a,b} + \omega_{a,b}}, \mu_{\pm} + \nu_{a,b} - \frac{1}{2} \sqrt{\mathcal{E}_{a,b} + \omega_{a,b}}; 1 \pm \frac{1}{2}; \tanh^2 x\right), \quad (17a) \end{aligned}$$

⁴It can be seen that both values of $\nu_{a,b}$ lead to the same solution in z space; we will use the negative sign for convenience in the analysis of the boundary conditions.

and for the reciprocal biquadratic mass,

$$\begin{aligned}\psi_{a,b}^{\pm}(x) &= x^{2\mu_{\pm}}(1+x^2)^{-\left(\mu_{\pm}+\nu_{a,b}+\frac{1}{2}\right)} {}_2F_1\left(\alpha_{a,b}^{\pm}, \beta_{a,b}^{\pm}; \gamma_{\pm}; \frac{x^2}{1+x^2}\right) \\ &= x^{2\mu_{\pm}}(1+x^2)^{-\left(\mu_{\pm}+\nu_{a,b}+\frac{1}{2}\right)} \times \\ &\times {}_2F_1\left(\mu_{\pm} + \nu_{a,b} + \frac{1}{2}\sqrt{\mathcal{E}_{a,b} + \omega_{a,b}}, \mu_{\pm} + \nu_{a,b} - \frac{1}{2}\sqrt{\mathcal{E}_{a,b} + \omega_{a,b}}; 1 \pm \frac{1}{2}; \frac{x^2}{1+x^2}\right). \quad (17b)\end{aligned}$$

Eqs. (17) show that if we compare two orderings having the same value of $\omega_{a,b}$ (as the ZK and LK orderings with soliton-like mass, or the ZK and MM orderings with reciprocal biquadratic mass) the wave functions distinguish themselves only by $\mathcal{E}_{a,b}$. Therefore, in this case, if we choose energy levels such that $\tilde{E} - V_{a,b}^{(0)}$ is the same for the two Hamiltonians, the solutions for both orderings will be also identical.

3.1.3 The energy spectra

The z space solutions must obey the boundary conditions $\zeta_{a,b}\left(\pm\frac{\pi}{2}\right) = 0$. We distinguish three cases depending on the sign of $\omega_{a,b}$. As resulting from the squeeze theorem we have $\lim_{|z|\rightarrow\frac{\pi}{2}^-}(\cos z)^{2\nu_{a,b}} = 0$ for $\omega_{a,b} < 0$, 1 for $\omega_{a,b} = 0$ and ∞ for $\omega_{a,b} > 0$, and thus, for $\omega_{a,b} \geq 0$ we must impose ${}_2F_1\left(\alpha_{a,b}^{\pm}, \beta_{a,b}^{\pm}; \gamma_{\pm}; 1\right) = 0$. This is the case of MM and BDD orderings for the soliton-like mass and of BDD, ZK and MM orderings for the reciprocal biquadratic mass. When $\Re\left(\gamma_{\pm} - \alpha_{a,b}^{\pm} - \beta_{a,b}^{\pm}\right) = \Re\left(\frac{1}{2}\sqrt{1+4\omega_{a,b}}\right) > 0$, we can use Gauss summation theorem [59] to rewrite

$${}_2F_1\left(\alpha_{a,b}^{\pm}, \beta_{a,b}^{\pm}; \gamma_{\pm}; 1\right) = \frac{\Gamma\left(1 \pm \frac{1}{2}\right)\Gamma\left(\frac{1}{2}\sqrt{1+4\omega_{a,b}}\right)}{\Gamma\left(\gamma_{\pm} - \alpha_{a,b}^{\pm}\right)\Gamma\left(\gamma_{\pm} - \beta_{a,b}^{\pm}\right)}. \quad (18)$$

As a consequence, the boundary condition implies $\gamma_{\pm} - \alpha_{a,b}^{\pm} = -\ell$, $\ell \in \mathbb{Z}_+$ ($\ell = 0, 1, 2, \dots$) which, in turn, results in a discrete non-degenerate energy spectrum for the general solution. Such spectrum reads

$$\tilde{E}_{a,b;n} = n^2 + 2(1 - 2\nu_{a,b})n + 1 - 2\nu_{a,b} + V_{a,b}^{(0)}, \quad n \in \mathbb{Z}_+, \quad (19)$$

where $n \equiv 2\ell$ for the solutions $\psi_{a,b}^-(x)$ (even solutions) and $n \equiv 2\ell + 1$ for the solutions $\psi_{a,b}^+(x)$ (odd solutions). The ground state is given by $\tilde{E}_{a,b;0} = 1 - 2\nu_{a,b} + V_{a,b}^{(0)}$ which is greater than $V_{a,b}^{(0)}$ as expected.

On the other hand, for $\omega_{a,b} < 0$, the effective potentials are bottomless barriers and the boundary conditions are automatically respected for any energy level. The spectrum is determined by the

derivative $\zeta_{a,b}^{\pm \prime}(z)$ at the border

$$\lim_{z \rightarrow \pm \frac{\pi}{2}} \zeta_{a,b}^{\pm \prime}(z) = -2\nu_{a,b} {}_2F_1\left(\alpha_{a,b}^{\pm}, \beta_{a,b}^{\pm}; \gamma_{\pm}; 1\right) \lim_{z \rightarrow \pm \frac{\pi}{2}} (\cos z)^{2\nu_{a,b}-1} \quad (20)$$

which is divergent. Actually, for $-\frac{1}{4} < \omega_{a,b} < 0$ one can avoid the singularity by cancellation of an identical factor in the hypergeometric function. In this case we would get the same spectrum given by eq. (19). This is a highly unexpected result for a bottomless barrier seems to behave like an infinite potential well. The same cannot be done for $\omega_{a,b} \leq -\frac{1}{4}$ because the transcendental equation ${}_2F_1\left(\alpha_{a,b}^{\pm}, \beta_{a,b}^{\pm}; \gamma_{\pm}; 1\right) = 0$ has no solutions for \tilde{E} ; therefore the GW, ZK and LK orderings with soliton-like mass and GW and LK orderings with reciprocal biquadratic mass do not have physically acceptable states and must be discarded.

Now we can write the discrete eigenstates (even and odd) compactly in terms of ℓ :

$$\psi_{a,b;\ell}^{\pm}(x) = (\tanh x)^{2\mu_{\pm}} (\operatorname{sech} x)^{2\nu_{a,b} + \frac{1}{2}} {}_2F_1\left(2\mu_{\pm} + \frac{1}{2} + \ell, 2\nu_{a,b} - \frac{1}{2} - \ell; 1 \pm \frac{1}{2}; \tanh^2 x\right) \quad (21a)$$

for the soliton-like mass, and

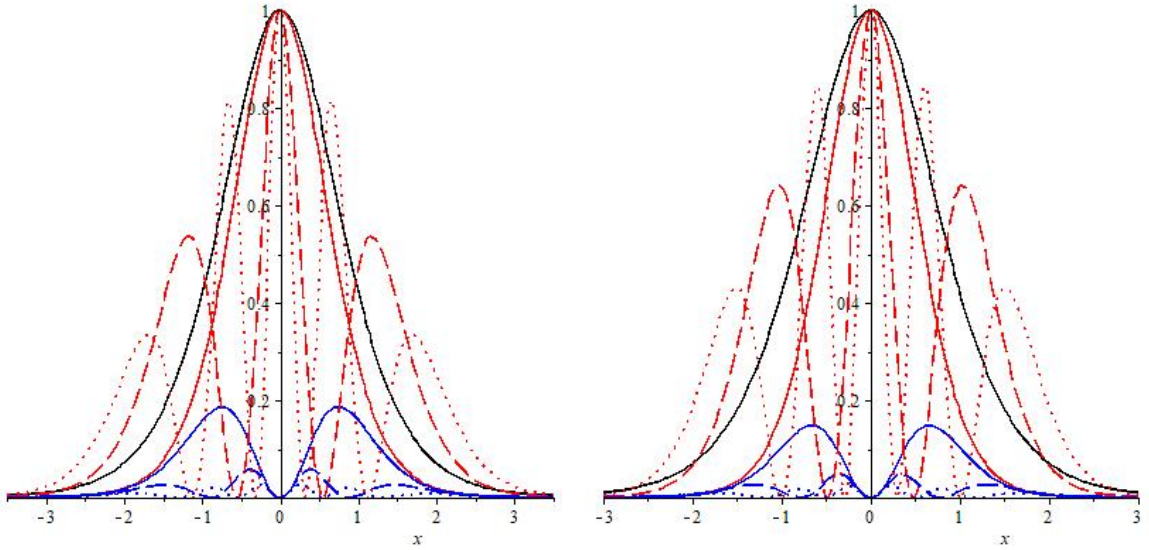
$$\psi_{a,b;\ell}^{\pm}(x) = x^{2\mu_{\pm}} (1+x^2)^{-\left(\mu_{\pm} + \nu_{a,b} + \frac{1}{2}\right)} {}_2F_1\left(2\mu_{\pm} + \frac{1}{2} + \ell, 2\nu_{a,b} - \frac{1}{2} - \ell; 1 \pm \frac{1}{2}; \frac{x^2}{1+x^2}\right) \quad (21b)$$

for the reciprocal biquadratic mass.

3.1.4 Graphics of the probability densities

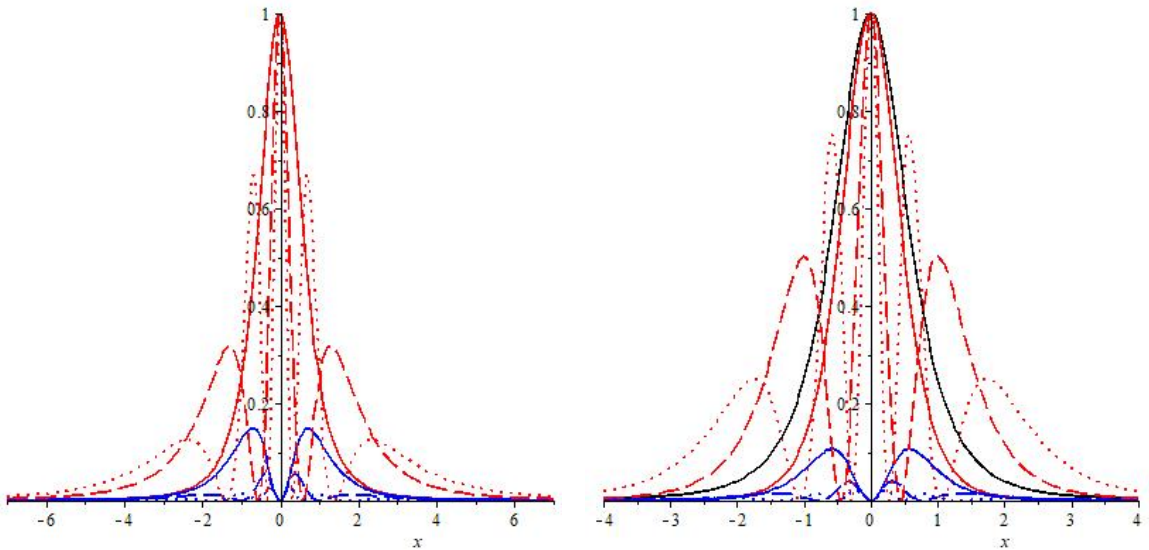
The probability densities associated with each particular solution, $\rho_{a,b}^{\pm}(x) \equiv \left|\psi_{a,b}^{\pm}(x)\right|^2$ and $\rho_{a,b;\ell}^{\pm}(x) \equiv \left|\psi_{a,b;\ell}^{\pm}(x)\right|^2$, are plotted in Figs. 2 and 3 (for the soliton-like and reciprocal biquadratic masses, respectively).

From Fig. 3(a) we can see that $\rho_{-1/2,-1/2;0}^{-}(x) = \rho_{-1/4,-1/4;0}^{-}(x) = m(x)$, which is easily verified algebraically using the identity ${}_2F_1(\alpha, \beta; \alpha; y) = (1-y)^{-\beta}$.



(a) Plots of $\rho_{-1/4,-1/4;l}^{\pm}(x)$ for $l = 0, 1$ and 2 (solid, dashed and dotted lines, respectively). (b) Plots of $\rho_{0,0;l}^{\pm}(x)$ for $l = 0, 1$ and 2 (solid, dashed and dotted lines, respectively).

Figure 2: Graphics of probability densities associated with the even (in red) and odd (in blue) unnormalized solutions for the soliton-like mass and for the (a) MM and (b) BDD orderings. The solid black line corresponds to $m(x) = \text{sech}^2 x$.



(a) Plots of $\rho_{-1/2,-1/2;l}^{\pm}(x)$ and $\rho_{-1/4,-1/4;l}^{\pm}(x)$ for $l = 0, 1$ and 2 (solid, dashed and dotted lines, respectively). (b) Plots of $\rho_{0,0;l}^{\pm}(x)$ for $l = 0, 1$ and 2 (solid, dashed and dotted lines, respectively).

Figure 3: Graphics of probability densities associated with the even (in red) and odd (in blue) unnormalized solutions for the reciprocal biquadratic mass and for the (a) ZK and MM and (b) BDD orderings. The solid black line corresponds to $m(x) = (1 + x^2)^{-2}$.

3.2 The reciprocal quadratic profile

Now we study the reciprocal quadratic mass [14, 23, 60–63],

$$M(x) = m_0 \left[1 + \left(\frac{x}{\epsilon} \right)^2 \right]^{-1} \Leftrightarrow m(x) = (1 + x^2)^{-1} . \quad (22)$$

3.2.1 The effective potential

For this mass, eq. (5a) results in

$$x = \sinh z , \quad (23)$$

mapping $\mathbb{R} \ni x \mapsto z \in \mathbb{R}$. The effective potential – eq. (6b) – is

$$V_{a,b}(z) = \omega_{a,b} \operatorname{sech}^2 z + V_{a,b}^{(\infty)} = V_{a,b}^{(0)} - \omega_{a,b} \tanh^2 z , \quad (24a)$$

where we define (see Table 2)

$$\omega_{a,b} \equiv \frac{1}{4} - 4ab \quad , \quad V_{a,b}^{(0)} \equiv V_{a,b}(0) = a + b + \frac{1}{2} \quad \text{and} \quad V_{a,b}^{(\infty)} \equiv V_{a,b}(\pm\infty) = 4ab + a + b + \frac{1}{4} . \quad (24b)$$

Table 2: Values of $\omega_{a,b}$, $V_{a,b}^{(0)}$ and $V_{a,b}^{(\infty)}$ for each ordering, for the reciprocal quadratic mass.

Orderings	$\omega_{a,b}$	$V_{a,b}^{(0)}$	$V_{a,b}^{(\infty)}$
BDD	1/4	1/2	1/4
GW	1/4	-1/2	-3/4
ZK	-3/4	-1/2	1/4
LK	1/4	0	-1/4
MM	0	0	0

We observe that $V_{a,b}(z)$ is a finite potential well when $\omega_{a,b} < 0$ and a finite barrier when $\omega_{a,b} > 0$; when $\omega_{a,b} = 0$, $V_{a,b}(z)$ is just uniform. Furthermore, since $V_{a,b}^{(0)} - V_{a,b}^{(\infty)} = \omega_{a,b}$, we can interpret $|\omega_{a,b}|$ as the amplitude of the potential well or barrier.

The graphics of $V_{a,b}(z)$ can be seen in Fig. 4.

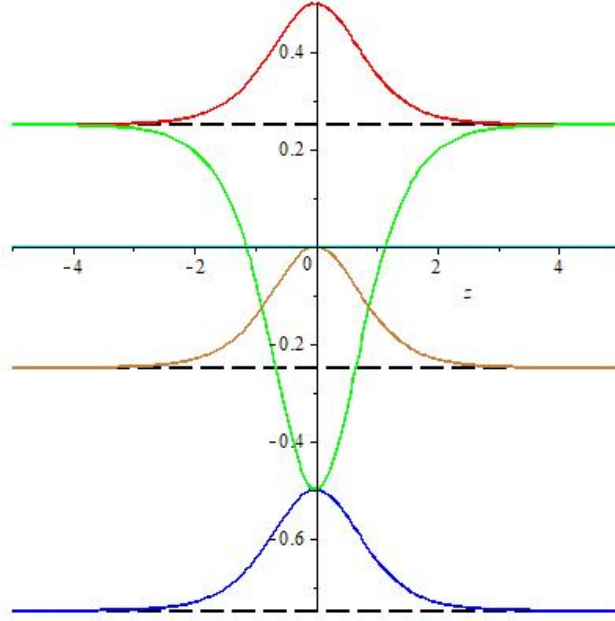


Figure 4: Graphics of $V_{a,b}(z)$ for the reciprocal quadratic profile and for the BDD, GW, ZK, LK and MM orderings (in red, blue, green, golden and cyan, respectively).

3.2.2 Solutions

We change variables again by defining

$$y = \tanh^2 z, \quad (25a)$$

mapping $\mathbb{R} \ni z \mapsto y \in [0, 1)$, and define a function $\xi(y)$ by

$$\zeta(z(y)) = y^\mu (1-y)^\nu \xi(y) \quad , \quad \mu, \nu \in \mathbb{C}. \quad (25b)$$

Thus, eq. (6a) becomes the following differential equation:

$$y(1-y)\xi''(y) + \left[2\mu + \frac{1}{2} - \left(2\mu + 2\nu + \frac{3}{2}\right)y\right]\xi'(y) + \left[\frac{\mu^2 - \frac{\mu}{2}}{y} + \frac{\nu^2 + \frac{\mathcal{E}_{a,b}}{4}}{1-y} - \frac{\omega_{a,b}}{4} - (\mu + \nu)^2 - \frac{\mu + \nu}{2}\right]\xi(y) = 0, \quad (26)$$

where we defined $\mathcal{E}_{a,b} \equiv \tilde{E} - V_{a,b}^{(\infty)}$. Thus $\mathcal{E}_{a,b}$ represents the energy levels measured with respect to value of the potential at infinite. In this case we choose μ and ν such that

$$\mu^2 - \frac{\mu}{2} = 0 \Rightarrow \mu_{\pm} = \frac{1 \pm 1}{4} \quad \text{and} \quad \nu^2 + \frac{\mathcal{E}_{a,b}}{4} = 0 \Rightarrow \nu_{a,b} = -\frac{1}{2}\sqrt{-\mathcal{E}_{a,b}}, \quad (27)$$

the above equation becomes

$$y(1-y)\xi''(y) + \left[2\mu_{\pm} + \frac{1}{2} - \left(2\mu_{\pm} + 2\nu_{a,b} + \frac{3}{2}\right)y\right]\xi'(y) - \left[(\mu_{\pm} + \nu_{a,b})^2 + \frac{\mu_{\pm} + \nu_{a,b}}{2} + \frac{\omega_{a,b}}{4}\right]\xi(y) = 0, \quad (28)$$

which is a Gauss hypergeometric equation with parameters

$$\gamma_{\pm} \equiv 2\mu_{\pm} + \frac{1}{2} = 1 \pm \frac{1}{2}, \quad \alpha_{a,b}^{\pm} \equiv \mu_{\pm} + \nu_{a,b} + \frac{1}{4} + \sqrt{ab} \quad \text{and} \quad \beta_{a,b}^{\pm} \equiv \mu_{\pm} + \nu_{a,b} + \frac{1}{4} - \sqrt{ab}. \quad (29)$$

Since $\gamma_{\pm} \notin \mathbb{Z}$, then for both values of μ the previous equation has the same two independent solutions of Subsection 3.1 around $y = 0$, $\xi_{a,b}^{\pm}(y)$ and $\bar{\xi}_{a,b}^{\pm}(y)$. Combined with eqs. (25), these yield the two independent solutions in z space,

$$\zeta_{a,b}^{\pm}(z) = (\tanh z)^{2\mu_{\pm}} (\operatorname{sech} z)^{2\nu_{a,b}} {}_2F_1\left(\alpha_{a,b}^{\pm}, \beta_{a,b}^{\pm}; \gamma_{\pm}; \tanh^2 z\right). \quad (30)$$

The solutions in x space are obtained by combining the eqs. (5b), (23) and (30):

$$\begin{aligned} \psi_{a,b}^{\pm}(x) &= x^{2\mu_{\pm}} (1+x^2)^{-\left(\mu_{\pm} + \nu_{a,b} + \frac{1}{4}\right)} {}_2F_1\left(\alpha_{a,b}^{\pm}, \beta_{a,b}^{\pm}; \gamma_{\pm}; \frac{x^2}{1+x^2}\right) \\ &= x^{2\mu_{\pm}} (1+x^2)^{-\left(\mu_{\pm} + \nu_{a,b} + \frac{1}{4}\right)} \times \\ &\quad \times {}_2F_1\left(\mu_{\pm} + \nu_{a,b} + \frac{1}{4} + \sqrt{ab}, \mu_{\pm} + \nu_{a,b} + \frac{1}{4} - \sqrt{ab}; 1 \pm \frac{1}{2}; \frac{x^2}{1+x^2}\right). \end{aligned} \quad (31)$$

Once again, when we compare two orderings for which $\omega_{a,b}$ are equal (the case of BDD, GW and LK orderings), the solutions are distinguished by the value of $\mathcal{E}_{a,b}$. Therefore, if for such orderings we measure the energy levels with respect to $V_{a,b}^{(\infty)}$, the solutions are identical. Interestingly, for $\nu_{a,b} = \frac{1}{2}\sqrt{-\mathcal{E}_{a,b}}$, we would be led to equivalent results.

3.2.3 The energy spectra

In this case the normalization condition for $\zeta_{a,b}(z)$ demands $\zeta_{a,b}^{\pm}(\pm\infty) < \infty$. Since $\lim_{z \rightarrow \pm\infty} (\operatorname{sech} z)^{2\nu_{a,b}}$ is undefined for $\mathcal{E}_{a,b} > 0$, equal to 1 for $\mathcal{E}_{a,b} = 0$ and infinity for $\mathcal{E}_{a,b} < 0$, we can separate our analysis in the following three cases:

1. $\mathcal{E}_{a,b} > 0 \Leftrightarrow \tilde{E} > V_{a,b}^{(\infty)}$ (scattering states): $\zeta_{a,b}(z)$ oscillates indefinitely, modulated by ${}_2F_1\left(\alpha_{a,b}^{\pm}, \beta_{a,b}^{\pm}; \gamma_{\pm}; \tanh^2 z\right)$, but $\psi_{a,b}(x)$ is normalizable because

$$\lim_{x \rightarrow \pm\infty} m^{1/4} = \lim_{x \rightarrow \pm\infty} (1+x^2)^{-1/4} = 0. \quad (32)$$

The energy spectrum is continuous;

2. $\mathcal{E}_{a,b} = 0 \Leftrightarrow \tilde{E} = V_{a,b}^{(\infty)}$ (trivial state): $\zeta_{a,b}(z)$ reduces to the trivial solution and is thus irrelevant;
3. $\mathcal{E}_{a,b} < 0 \Leftrightarrow \tilde{E} < V_{a,b}^{(\infty)}$ (bound states): in this case we must impose that ${}_2F_1\left(\alpha_{a,b}^\pm, \beta_{a,b}^\pm; \gamma_\pm; 1\right) = 0$ and, therefore, since $\Re\left(\gamma_\pm - \alpha_{a,b}^\pm - \beta_{a,b}^\pm\right) = \Re\left(\sqrt{-\mathcal{E}_{a,b}}\right) > 0$, we can use again the Gauss summation theorem and take $\gamma_\pm - \alpha_{a,b}^\pm = -\ell$, $\ell \in \mathbb{Z}_+$ ($\ell = 0, 1, 2, \dots$). With this we obtain, for the general solution, a discrete non-degenerate energy spectrum

$$\tilde{E}_{a,b;n} = -n^2 + \left(4\sqrt{ab} - 1\right)n + 2\sqrt{ab} - \frac{1}{2} + V_{a,b}^{(0)}, \quad (33a)$$

where $n \equiv 2\ell$ for the solutions $\psi_{a,b}^-(x)$ (even solutions) and $n \equiv 2\ell + 1$ for the solutions $\psi_{a,b}^+(x)$ (odd solutions). We also verify that these states are restricted to the interval

$$0 \leq n < 2\sqrt{ab} - \frac{1}{2} \Leftrightarrow 0 \leq \ell < \sqrt{ab} - \mu_\pm - \frac{1}{4}. \quad (33b)$$

Put in terms of $\omega_{a,b}$:

- when $\omega_{a,b} \geq 0$, solutions are all of scattering type;
- when $-2 \leq \omega_{a,b} < 0$, there is only one bound state (the ground state), all the others are of scattering type;
- when $\omega_{a,b} < -2$, both bound and scattering states exist, and the general solution is given by the LC of both particular solutions.

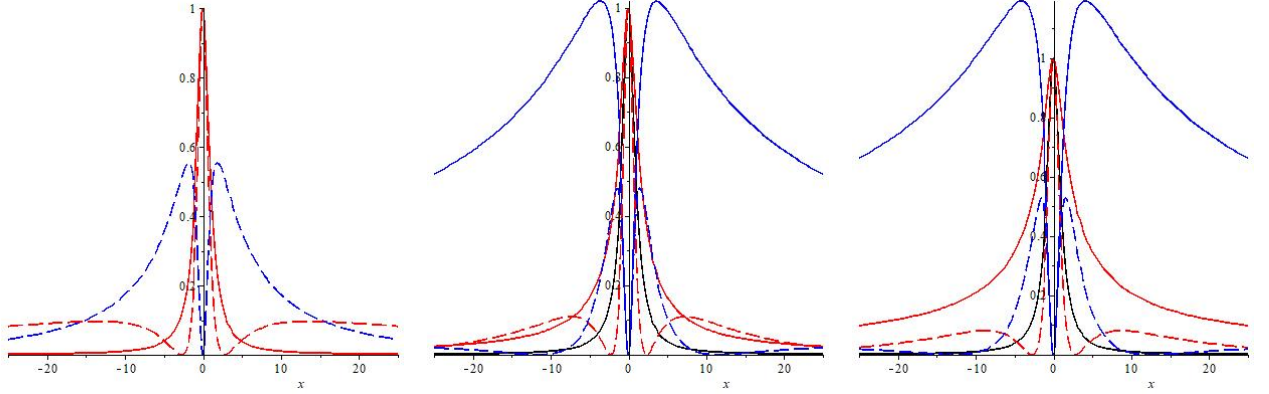
Synthesizing, when the effective potential is a finite barrier ($\omega_{a,b} > 0$) or uniform ($\omega_{a,b} = 0$), there are no bound states. On the other hand, when the effective potential is a finite well ($\omega_{a,b} < 0$), the bound states are discretized, with energy levels given by eqs. (33). Written in terms of ℓ , eq. (31) reads

$$\begin{aligned} \psi_{a,b;\ell}^\pm(x) &= x^{2\mu_\pm} (1+x^2)^{-\left(\ell+2\mu_\pm+\frac{1}{2}-\sqrt{ab}\right)} \times \\ &\quad \times {}_2F_1\left(\ell+2\mu_\pm+\frac{1}{2}, \ell+2\mu_\pm+\frac{1}{2}-2\sqrt{ab}; 1 \pm \frac{1}{2}; \frac{x^2}{1+x^2}\right). \end{aligned} \quad (34)$$

In this case, when we compare two orderings that have the same $\omega_{a,b}$, the solutions can be distinguished by the values of ℓ .

3.2.4 Graphics of the probability densities

For this mass profile, the ZK ordering is the only one having bound states; more specifically, just the ground state⁵ (the graphics of both $\rho_{-1/2,-1/2;0}^-(x)$ and $\rho_{-1/2,-1/2}^\pm(x)$ for $\tilde{E} = 1/2$ are plotted in Fig. 5(a)). For the other orderings the graphics of $\rho_{a,b}^\pm(x)$ are plotted in Figs. 5(b) and 5(c); in this case the BDD, ZK and LK orderings fit the same figure.



(a) Graphics of $\rho_{-1/2,-1/2;0}^-(x)$ (solid red line) and of $\rho_{-1/2,-1/2}^\pm(x)$ for $\tilde{E} = 1/32$ and 1 (solid and dashed lines, respectively). (b) Graphics of $\rho_{-1/4,-1/4}^\pm(x)$ for $\tilde{E} = 1/32$ and 1 (solid and dashed lines, respectively). (c) Graphics of $\rho_{0,0}^\pm(x)$, $\rho_{-1,0}^\pm(x)$ and $\rho_{0,-1/2}^\pm(x)$ for $\tilde{E} = V_{a,b}^{(\infty)} + 1/32$ and $V_{a,b}^{(\infty)} + 1$ (solid and dashed lines, respectively).

Figure 5: Graphics of the probability densities associated to even (in red) and odd (in blue) unnormalized solutions for the reciprocal quadratic mass and for the (a) ZK, (b) MM and (c) BDD, GW and LK orderings. The solid black line is for the curve $m(x) = (1 + x^2)^{-1}$.

In Fig. 5(a) we verify that $\rho_{-1/2,-1/2;0}^-(x) = m(x)$, which can be verified using the identity ${}_2F_1(\alpha, \beta; \alpha; y) = (1 - y)^{-\beta}$.

3.3 The exponential profile

Let us take the following exponential profile [45, 58, 64]:

$$M(x) = m_0 e^{-2|x|/\epsilon} \Leftrightarrow m(x) = e^{-2|x|}, \quad (35)$$

which vanishes asymptotically in both directions.

⁵See Table 2 and compare with eqs. (33)

3.3.1 The effective potential

In this case eq. (5a) implies the relationship

$$e^{-|x|} = 1 - |z|, \quad (36)$$

mapping $\mathbb{R} \ni x \mapsto z \in (-1, 1)$. The integration constants for each branch were chosen in such a way that $\mathbb{R}_-^* \ni x \mapsto z \in (-1, 0)$ and $\mathbb{R}_+ \ni x \mapsto z \in [0, 1)$. The effective potential – eq. (6b) – is

$$V_{a,b}(z) = \frac{\omega_{a,b}}{(1 - |z|)^2}, \quad \omega_{a,b} \equiv 4ab + 2(a + b) + \frac{3}{4}, \quad (37)$$

which is continuous throughout the domain (interestingly, $\omega_{a,b}$ is the same one found for the soliton-like profile). When $\omega_{a,b} \neq 0$ it has a critical point $V_{a,b}(0) = \omega_{a,b}$ and two singularities, at $z = \pm 1$, which depend on the signal of $\omega_{a,b}$: if $\omega_{a,b} > 0$ then $V_{a,b}(z)$ is an infinite well; if $\omega_{a,b} < 0$ it is bottomless barrier.

It is easy to see that when different orderings have the same value of $\omega_{a,b}$ (as is the case with the ZK and LK orderings) they also share the same effective potential and therefore we expect the same solutions for the same energies.

The graphics of $V_{a,b}(z)$ can be seen in Fig. 6.

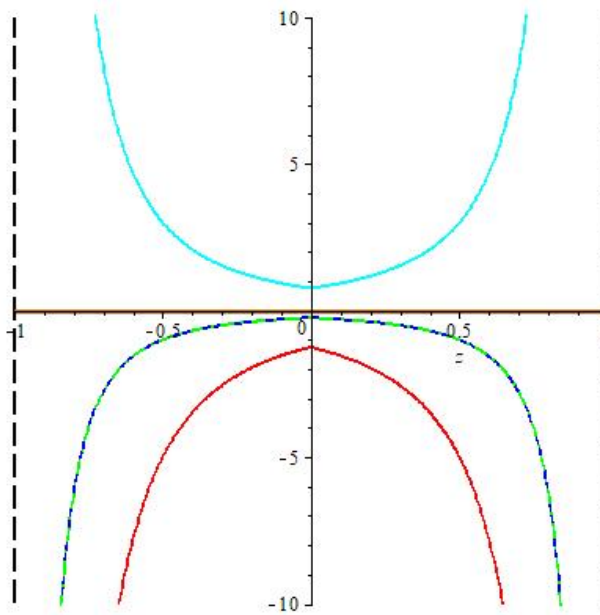


Figure 6: Graphics of $V_{a,b}(z)$ referring to the exponential mass for the GW, ZK, LK, MM and BDD orderings (in red, blue, green, golden and cyan, respectively). Note the overlap between $V_{-1/2,-1/2}(z)$ and $V_{0,-1/2}(z)$

3.3.2 Solutions

This time we change the variables by

$$y = \nu(1 - |z|) \quad , \quad \nu \in \mathbb{C}^* \quad , \quad (38a)$$

mapping $(-1, 1) \ni z \mapsto y \in \{y \in \mathbb{C}^*, |y| \leq |\nu|\}$ (at the perimeter $|y| = |\nu|$ ($z = 0$), the solutions in z space can be obtained by continuity) and define a function $\xi(y)$ such that

$$\zeta(z(y)) = \left(\frac{y}{\nu}\right)^{1/2} \xi(y) \quad . \quad (38b)$$

With this, eq. (6a) transforms into⁶

$$y^2 \xi''(y) + y \xi'(y) + \left(\frac{\tilde{E}}{\nu^2} y^2 - \alpha_{a,b}^2\right) \xi(y) = 0 \quad , \quad \alpha_{a,b} \equiv \frac{1}{2} \sqrt{1 + 4\omega_{a,b}} \in \mathbb{R}_+ \cup \mathbb{I}_+^* \quad . \quad (39a)$$

Choosing $\nu = \sqrt{\tilde{E}}$ for $\tilde{E} \neq 0$, and $\nu = 1$ for $\tilde{E} = 0$, the above equation becomes

$$\begin{cases} y^2 \xi''(y) + y \xi'(y) + (y^2 - \alpha_{a,b}^2) \xi(y) = 0 & \tilde{E} \neq 0 \\ y^2 \xi''(y) + y \xi'(y) - \alpha_{a,b}^2 \xi(y) = 0 & \tilde{E} = 0 \end{cases} \quad , \quad (39b)$$

the first line is equivalent to a regular Bessel's equation of order $\alpha_{a,b}$ and the second to a 2nd order homogeneous Euler-Cauchy equation.

The two independent solutions of each differential equation are

$$\xi_{a,b}^{(1)}(y) = \begin{cases} J_{\alpha_{a,b}}(y) & \tilde{E} \neq 0 \\ y^{\alpha_{a,b}} & \tilde{E} = 0 \end{cases} \quad \text{and} \quad \xi_{a,b}^{(2)}(y) = \begin{cases} H_{\alpha_{a,b}}^{(1)}(y) & \tilde{E} \neq 0 \\ \begin{cases} y^{-\alpha_{a,b}} & \alpha_{a,b} \neq 0 \\ \ln y & \alpha_{a,b} = 0 \end{cases} & \tilde{E} = 0 \end{cases} \quad , \quad (40)$$

where $J_\alpha(y)$ and $H_\alpha^{(1)}(y)$ are, respectively, the 1st kind Bessel and Hankel functions of order α . Combining them with the eqs. (38) we obtain the solutions in z space:

$$\zeta_{a,b}^{(1)}(z) = \begin{cases} \sqrt{1 - |z|} J_{\alpha_{a,b}}(\sqrt{\tilde{E}}(1 - |z|)) & \tilde{E} \neq 0 \\ (1 - |z|)^{\frac{1}{2} + \alpha_{a,b}} & \tilde{E} = 0 \end{cases} \quad (41a)$$

⁶Here, \mathbb{I}_+^* denotes the set of elements written in the form ih , where $h \in \mathbb{R}_+^*$.

and

$$\zeta_{a,b}^{(2)}(z) = \begin{cases} \sqrt{1-|z|} H_{\alpha_{a,b}}^{(1)}\left(\sqrt{\tilde{E}}(1-|z|)\right) & \tilde{E} \neq 0 \\ \begin{cases} (1-|z|)^{\frac{1}{2}-\alpha_{a,b}} & \alpha_{a,b} \neq 0 \\ \sqrt{1-|z|} \ln(1-|z|) & \alpha_{a,b} = 0 \end{cases} & \tilde{E} = 0 \end{cases} . \quad (41b)$$

3.3.3 The energy spectra

The general solution in z space, $\zeta_{a,b}(z)$, must obey the conditions $\zeta_{a,b}(\pm 1) = 0$ and $\zeta'_{a,b}(0) = 0$ (the second one is obtained from continuity of wave function derivative; note in eqs. (41) that functions are even).

Taking into account the asymptotic behavior of Bessel functions for small arguments and with the aid of identity

$$C'_\alpha(y) = C_{\alpha-1}(y) - \frac{\alpha}{y} C_\alpha(y) , \quad (42)$$

where $C_\alpha(y)$ denotes the functions $J_\alpha(y)$ or $H_\alpha^{(1)}(y)$, we conclude that when $\alpha_{a,b} \in \mathbb{N}_+^* \Leftrightarrow \omega_{a,b} < -\frac{1}{4}$ there is no solution meeting the above conditions. On the other hand, when $\alpha_{a,b} \geq 0 \Leftrightarrow \omega_{a,b} \geq -\frac{1}{4}$ only eq. (41a) is a physically valid solution. It presents a discrete energy spectrum $\tilde{E}_{a,b;n} \equiv k_{a,b;n}^2$, where $k_{a,b;n} > 0$ is the n th positive solution of the transcendental equation

$$2k_{a,b} J_{\alpha_{a,b}-1}(k_{a,b}) + (1 - 2\alpha_{a,b}) J_{\alpha_{a,b}}(k_{a,b}) = 0 , \quad (43)$$

Since the exchange $k_{a,b;n} \rightarrow -k_{a,b;n}$ produces the same energy spectrum, we find that the eigenstates show double degeneracy.

In the x space the solutions are obtained by combining the eqs. (5b), (36) and (41), considering eq. (43)

$$\psi_{a,b;n}(x) = e^{-|x|} J_{\alpha_{a,b}}(k_{a,b;n} e^{-|x|}) \quad , \quad n \in \mathbb{Z}_+^* \quad , \quad \omega_{a,b} \geq -\frac{1}{4} . \quad (44)$$

Looking at eq. (44) we see that eigenstates can be distinguished from each other by the ordering, represented by $\alpha_{a,b}$, as well as the energy level $\tilde{E}_{a,b;n} \equiv k_{a,b;n}^2$. Thus, the eigenstates with same energy are indistinguishable between two orderings with the same $\omega_{a,b}$, as expected.

The value of $k_{a,b;n} = \sqrt{\tilde{E}_{a,b;n}}$ can be calculated numerically for each ordering with $\omega_{a,b} \geq -\frac{1}{4}$ from eq. (43) (see Table 3).

Table 3: Three first values of $k_{a,b;n}$ for the BDD, ZK/LK and MM orderings. The GW ordering has no valid solutions.

Orderings	$k_{a,b;n}$		
	$n = 1$	$n = 2$	$n = 3$
ZK/LK	0.9407705639	3.959371185	7.086380848
MM	1.570796327	4.712388980	7.853981634
BDD	2.165871271	5.427433202	8.595426306

It is worth noting that a system with exponential mass has only bound states, even for orderings with $-\frac{1}{4} \leq \omega_{a,b} < 0$, corresponding to potentials $V_{a,b}(z)$ which are bottomless barriers. This contradicts the common sense that there should be only scattering states and a continuous and inferiorly unlimited spectrum. As we can see, in this case a bottomless barrier behaves like infinite potential well.

The GW ordering is automatically removed for having no valid solution.

3.3.4 Graphics of the probability densities

The graphics of $\rho_{a,b;n}(x) \equiv |\psi_{a,b;n}(x)|^2$ are potted in Fig. 7. The probability densities associated with ZK and LK orderings are plotted in a same picture because they are identical.

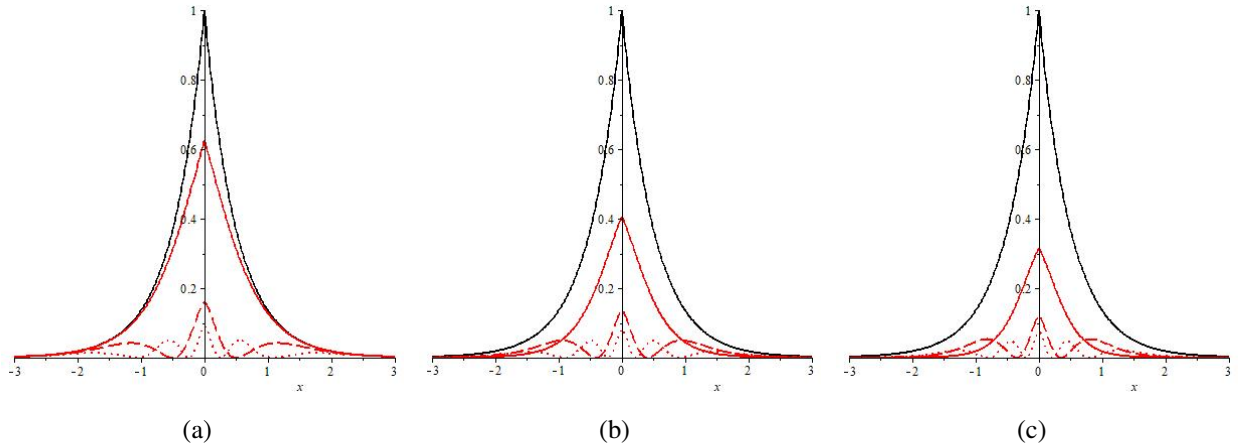


Figure 7: Graphics of the probability densities associated with eq. (44) (unnormalized solutions) for the exponential mass and for the (a) ZK and LK, (b) MM and (c) BDD orderings, with $n = 1, 2$ and 3 (solid, dashed and dotted lines, respectively). The solid black line corresponds to $m(x) = e^{-2|x|}$.

Fig. 7 shows that although solutions in z space have continuous derivatives, this is not true for solutions in x space. In fact, taking the derivative of eq. (44) and considering eq. (43) we conclude

that

$$\lim_{x \rightarrow 0^\pm} \psi'_{a,b;n}(x) = \pm \frac{1}{k_{a,b;n}} \left(\frac{1}{2} - k_{a,b;n} \right) J_{\alpha_{a,b}}(k_{a,b;n}) , \quad (45)$$

i.e., the derivatives of the solutions are continuous at the origin only if $k_{a,b;n} = \frac{1}{2}$ or if $k_{a,b;n}$ is some zero of the 1st type Bessel function, which is not necessarily true.

3.4 The parabolic profile

Let us focus on the analysis of a parabolic mass density [23, 65, 66],

$$M(x) = m_0 \left(\frac{2x}{\epsilon} \right)^2 \Leftrightarrow m(x) = 4x^2 . \quad (46)$$

Since it is an indefinitely growing profile, we restrict it to a finite region $|x| < \ell$, $\ell > 0$ which could possibly represent a heterostructure. This leaves the solutions free of boundary conditions.

3.4.1 The effective potential

For this mass, eq. (5a) results in the transformation

$$x^2 = |z| , \quad (47)$$

mapping $(-\ell, \ell) \ni x \mapsto z \in (-\ell^2, \ell^2)$. Eq. (5b) gives the effective potential

$$V_{a,b}(z) = \frac{\omega_{a,b}}{z^2} , \quad \omega_{a,b} \equiv ab + \frac{3}{4}(a+b) + \frac{5}{16} . \quad (48)$$

We observe that this expression is similar to the exponential mass effective potential under transformation $1 - |z| \rightarrow |z|$, (and a different $\omega_{a,b}$). Therefore, some analogous considerations can be made. Indeed, depending on the sign of $\omega_{a,b}$ the potential will behave very differently: if $\omega_{a,b} > 0$ ($\omega_{a,b} < 0$) then the potential is an infinite barrier (bottomless well) because it diverges to $+\infty$ ($-\infty$) at the origin. The plots of the effective potentials for the different orderings are in Fig. 8.

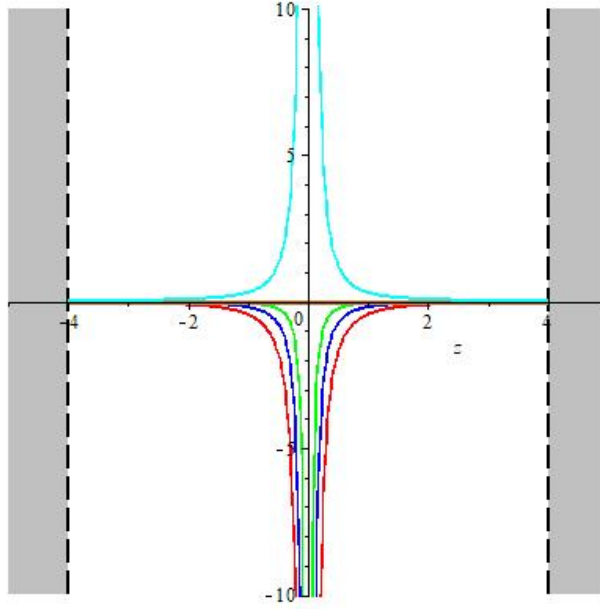


Figure 8: Shape of the effective potentials $V_{a,b}(z)$ for the GW ($\omega_{-1,0} = -7/16$), ZK ($\omega_{-1/2,-1/2} = -3/16$), LK ($\omega_{0,-1/2} = -1/16$), MM ($\omega_{-1/4,-1/4} = 0$) and BDD ($\omega_{0,0} = 5/16$) orderings (in red, blue, green, golden and cyan, respectively) and related to a system restricted, in x space, to the interval $|x| \leq 2$.

3.4.2 Solutions

The resemblance in z space of this with the exponential mass system allows the recognition of eqs. (41) as solutions for this case. We just need to make $1 - |z| \rightarrow |z|$ and substitute the definition of $\omega_{a,b}$ (the $\alpha_{a,b}$ and $\omega_{a,b}$ parameters are still related by $\alpha_{a,b} = \frac{1}{2}\sqrt{1 + 4\omega_{a,b}}$).

The analysis of the solutions and their derivatives at the origin, show that there is no solution for $\alpha_{a,b} \in \mathbb{N}_+^* \cup \left[0, \frac{1}{2}\right) \Leftrightarrow \omega_{a,b} < 0$, which means that the orderings whose effective potentials in z space are bottomless wells are automatically excluded for this profile. When $\alpha_{a,b} = \frac{1}{2} \Leftrightarrow \omega_{a,b} = 0$ only the first solution with zero energy is acceptable, and it is reduced to $\zeta_{a,b}(z) = 1$. On the other hand, for $\alpha_{a,b} > \frac{1}{2} \Leftrightarrow \omega_{a,b} > 0$ just the first solution and their derivative converge and are continuous at $z = 0$. Thus, for positive $\omega_{a,b}$ parameters the physically acceptable solutions are

$$\zeta_{a,b}(z) = \begin{cases} \sqrt{|z|} J_{\alpha_{a,b}}(\sqrt{\tilde{E}}|z|) & \tilde{E} \neq 0 \\ |z|^{\frac{1}{2} + \alpha_{a,b}} & \tilde{E} = 0 \end{cases}, \quad \alpha_{a,b} > \frac{1}{2}. \quad (49)$$

which combined with eqs. (5b), (47) result in the x space eigenstates

$$\psi_{a,b}(x) = \begin{cases} |x|^{3/2} J_{\alpha_{a,b}}(\sqrt{\tilde{E}}x^2) & \tilde{E} \neq 0 \\ |x|^{\frac{3}{2}+2\alpha_{a,b}} & \tilde{E} = 0 \end{cases}, \quad \omega_{a,b} > 0. \quad (50)$$

3.4.3 The energy spectra

If we consider a heterostructure model with arbitrary mass and/or external potential in $|x| > \ell$, we can study how the potentials $V_{a,b}(z)$ behave in the region $|z| > \ell^2$. Then, we will be able to find energy levels and eventually evaluate the conditions for discretization or degeneracy resulting from

$$\lim_{z \rightarrow \pm\ell^\pm} \zeta_{a,b}(z) \text{ and } \lim_{z \rightarrow \pm\ell^\pm} \zeta'_{a,b}(z).$$

For example, if we assume that in $|x| > \ell$ the mass is uniform and the external potential is still zero, then $V_{a,b}(z) = 0$ in $|z| > \ell^2$ and solutions will be all free scattering states. If instead the mass has positive concavity out of the interval $(-\ell^2, \ell^2)$ the effective potential will result in a potential well and it will be possible to have bound states with negative energy above its minimum.

3.4.4 Graphics of the probability densities

The plots of the probability densities for the BDD ordering are shown in Fig. 9. The previous discussion gives us a plausible reason to illustrate at least one situation with negative eigenenergy. In any case, the displayed sector ($|x| < \ell$) shows tunneling states across the potential for parabolic mass distribution and BDD ordering.

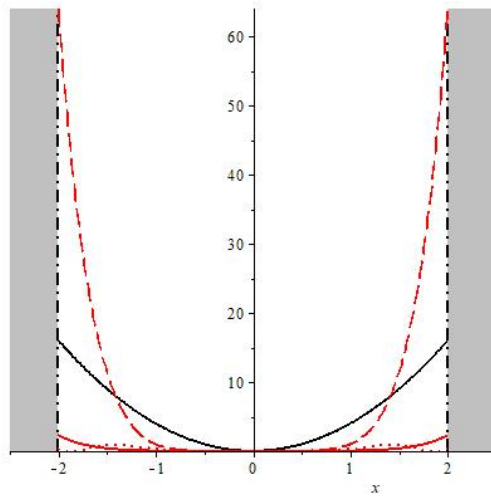


Figure 9: Graphics of BDD $\rho_{0,0}(x)$ for $\tilde{E} = -1/32, 0$ and 1 (solid, dashed and dotted red line, respectively). The solid black line corresponds to $m(x) = 4x^2$. The other orderings are not acceptable.

4 Double heterostructure: an example

In order to apply our previous results, we will consider a model of a one-dimensional quantum heterostructure where a charge carrier among two regions has a PDM of parabolic type. The particle mass changes from $m_0 m_1$ to $m_0 m_2$, $m_{1,2} > 0$, along an intermediate region IR of size 2ℓ symmetric about the origin:

$$M(x) = \begin{cases} m_0 m_1 & \frac{x}{\epsilon} < -\ell \\ 4m_0 \eta \left(\frac{x}{\epsilon} + \chi \right)^2 & \left| \frac{x}{\epsilon} \right| \leq \ell \\ m_0 m_2 & \frac{x}{\epsilon} > \ell \end{cases} \Leftrightarrow m = \begin{cases} m_1 & x < -\ell \\ 4\eta(x + \chi)^2 & |x| \leq \ell \\ m_2 & x > \ell \end{cases}, \quad (51)$$

with $\chi = \frac{\sqrt{m_2} + \sqrt{m_1}}{\sqrt{m_2} - \sqrt{m_1}} \ell$ and $\eta = \frac{(\sqrt{m_2} - \sqrt{m_1})^2}{16\ell^2}$.

4.1 Solutions

For $|x| > \ell$ the mass is constant and the solutions are the well-known ordinary wavefunctions

$$\psi(x) = \begin{cases} A e^{|k_1|x} & x < -\ell \\ B e^{-|k_2|x} & x > \ell \end{cases} \quad \tilde{E} < 0 \quad (52a)$$

and

$$\psi(x) = \begin{cases} A e^{ik_1 x} + A R e^{-ik_1 x} & x < -\ell \\ A T e^{ik_2 x} & x > \ell \end{cases} \quad \tilde{E} > 0 \quad (52b)$$

where $A, B, R, T \in \mathbb{C}$ (R and T are associated with reflection and transmission coefficients) and $k_{1,2} \equiv (m_{1,2} \tilde{E})^{1/2}$. In the IR the particular solutions $\psi_{a,b}^{(1,2)}(x)$ are those obtained in the previous section, with $x \rightarrow x + \chi$ and $\tilde{E} \rightarrow \eta \tilde{E}$. Now, the boundary conditions allow two independent components and the general solution inside is $\psi_{a,b}^{\text{in}}(x)$ in $|x| \leq \ell$, given by $\psi_{a,b}^{\text{in}}(x) = C^{(1)} \psi_{a,b}^{(1)}(x) + C^{(2)} \psi_{a,b}^{(2)}(x)$, with $C^{(1,2)} \in \mathbb{C}$ and

$$\psi_{a,b}^{(1)}(x) = \begin{cases} |x + \chi|^{3/2} I_{\alpha_{a,b}} \left((\eta |\tilde{E}|)^{1/2} (x + \chi)^2 \right) & \tilde{E} < 0 \\ |x + \chi|^{3/2} J_{\alpha_{a,b}} \left((\eta \tilde{E})^{1/2} (x + \chi)^2 \right) & \tilde{E} > 0 \end{cases} \quad (53a)$$

and

$$\psi_{a,b}^{(2)}(x) = \begin{cases} |x + \chi|^{3/2} K_{\alpha_{a,b}} \left((\eta |\tilde{E}|)^{1/2} (x + \chi)^2 \right) & \tilde{E} < 0 \\ |x + \chi|^{3/2} H_{\alpha_{a,b}}^{(1)} \left((\eta \tilde{E})^{1/2} (x + \chi)^2 \right) & \tilde{E} > 0 \end{cases}, \quad (53b)$$

where we have chosen to write these solutions in terms of modified Bessel functions.

4.2 Boundary conditions

The boundary conditions are defined by imposing the continuity of $\psi_{a,b}(x)$ and $\psi'_{a,b}(x)$. We can write these conditions in a compact way as follows. Define the following column vectors

$$\mathfrak{g}_{a,b;\tau} \equiv \begin{pmatrix} \psi_{a,b}^{(1)}((-1)^\tau \ell) \\ \psi_{a,b}^{(2)}((-1)^\tau \ell) \end{pmatrix}, \quad \dot{\mathfrak{g}}_{a,b;\tau} \equiv \begin{pmatrix} \psi_{a,b}^{(1)' }((-1)^\tau \ell) \\ \psi_{a,b}^{(2)' }((-1)^\tau \ell) \end{pmatrix}, \quad \mathbf{C} \equiv \begin{pmatrix} \mathbf{C}^{(1)} \\ \mathbf{C}^{(2)} \end{pmatrix} \quad \text{and} \\ \boldsymbol{\kappa}_{a,b;\tau} \equiv \dot{\mathfrak{g}}_{a,b;\tau} - (-1)^\tau i k_\tau \mathfrak{g}_{a,b;\tau}, \quad (54)$$

where $\tau = 1, 2$. With $\gamma^{(1,2)} \in \mathbb{C}$, we also define

$$\begin{pmatrix} \gamma^{(1)} \\ \gamma^{(2)} \end{pmatrix}_\perp \equiv \begin{pmatrix} \gamma^{(2)} \\ -\gamma^{(1)} \end{pmatrix} = \begin{pmatrix} 0 & 1 \\ -1 & 0 \end{pmatrix} \begin{pmatrix} \gamma^{(1)} \\ \gamma^{(2)} \end{pmatrix}, \quad (55)$$

i.e., index \perp denotes a rotation of $\frac{\pi}{2}$ counter clockwise.

The boundary conditions imply

$$\begin{cases} \begin{pmatrix} \mathfrak{g}_{a,b;1}^T \\ \dot{\mathfrak{g}}_{a,b;1}^T \end{pmatrix} \mathbf{C} = A e^{-\ell |k_1|} \begin{pmatrix} 1 \\ |k_1| \end{pmatrix} \\ \begin{pmatrix} \mathfrak{g}_{a,b;2}^T \\ \dot{\mathfrak{g}}_{a,b;2}^T \end{pmatrix} \mathbf{C} = B e^{-\ell |k_2|} \begin{pmatrix} 1 \\ -|k_2| \end{pmatrix} \end{cases} \quad \tilde{E} < 0 \quad (56a)$$

and

$$\begin{cases} \begin{pmatrix} \mathfrak{g}_{a,b;1}^T \\ \dot{\mathfrak{g}}_{a,b;1}^T \end{pmatrix} \mathbf{C} = A e^{-i\ell k_1} \begin{pmatrix} 1 \\ i k_1 \end{pmatrix} + A R e^{i\ell k_1} \begin{pmatrix} 1 \\ -i k_1 \end{pmatrix} \\ \begin{pmatrix} \mathfrak{g}_{a,b;2}^T \\ \dot{\mathfrak{g}}_{a,b;2}^T \end{pmatrix} \mathbf{C} = A T e^{i\ell k_2} \begin{pmatrix} 1 \\ i k_2 \end{pmatrix} \end{cases} \quad \tilde{E} > 0 \quad (56b)$$

(T denoting transposition). For $\tilde{E} < 0$, eqs. (56a) yield B and $C^{(1,2)}$ in terms of A ,

$$C_{a,b} = -A_{a,b} e^{-\ell|k_1|} \frac{\boldsymbol{\kappa}_{a,b;1\perp}}{\dot{\boldsymbol{\vartheta}}_{a,b;1}^T \boldsymbol{\vartheta}_{a,b;1\perp}} \quad \text{and} \quad B_{a,b} = -A_{a,b} e^{\ell(|k_2| - |k_1|)} \frac{\boldsymbol{\vartheta}_{a,b;2}^T \boldsymbol{\kappa}_{a,b;1\perp}}{\dot{\boldsymbol{\vartheta}}_{a,b;1}^T \boldsymbol{\vartheta}_{a,b;1\perp}}. \quad (57a)$$

A will be determined by normalization, and the discrete energy levels will result from the following transcendental equation

$$\boldsymbol{\kappa}_{a,b;1}^T \boldsymbol{\kappa}_{a,b;2\perp} = 0. \quad (57b)$$

For $\tilde{E} > 0$ states, eqs. (56b) yield $C^{(1,2)}$, R and T em terms of the free incident wave amplitude A ,

$$C_{a,b} = -2Aik_1 e^{-i\ell k_1} \frac{\boldsymbol{\kappa}_{a,b;2\perp}}{\boldsymbol{\kappa}_{a,b;1}^T \boldsymbol{\kappa}_{a,b;2\perp}} \quad \text{and} \quad \begin{pmatrix} R_{a,b} \\ T_{a,b} \end{pmatrix} = -\frac{e^{-i\ell k_1}}{\boldsymbol{\kappa}_{a,b;1}^T \boldsymbol{\kappa}_{a,b;2\perp}} \begin{pmatrix} e^{-i\ell k_1} \left(\dot{\boldsymbol{\vartheta}}_{a,b;1}^T - ik_1 \boldsymbol{\vartheta}_{a,b;1}^T \right) \boldsymbol{\kappa}_{a,b;2\perp} \\ 2ik_1 e^{-i\ell k_2} \dot{\boldsymbol{\vartheta}}_{a,b;2}^T \boldsymbol{\vartheta}_{a,b;2\perp} \end{pmatrix}. \quad (58)$$

4.3 Results

In order to plot our results, we choose the mass parameters $m_1 = m_2/2 = 0.5$ and $\ell = 1$. We will consider $m_0 \approx m_e$, where m_e is the free electron mass, and $\epsilon \approx \mu m$ for a typical heterojunction among semiconductors. In this particular case there are no bound states since there is no solution to eq. (57b). Instead, we have scattering states and the study of the flux probability results in

$$\frac{|R_{a,b}|^2}{\sqrt{m_1}} + \frac{|T_{a,b}|^2}{\sqrt{m_2}} = \frac{1}{\sqrt{m_1}}. \quad (59)$$

In Fig. 10 we can see the behaviour of $|R_{a,b}|^2$ and $|T_{a,b}|^2$ with respect to the energy, and verify the validity of eq. (59).

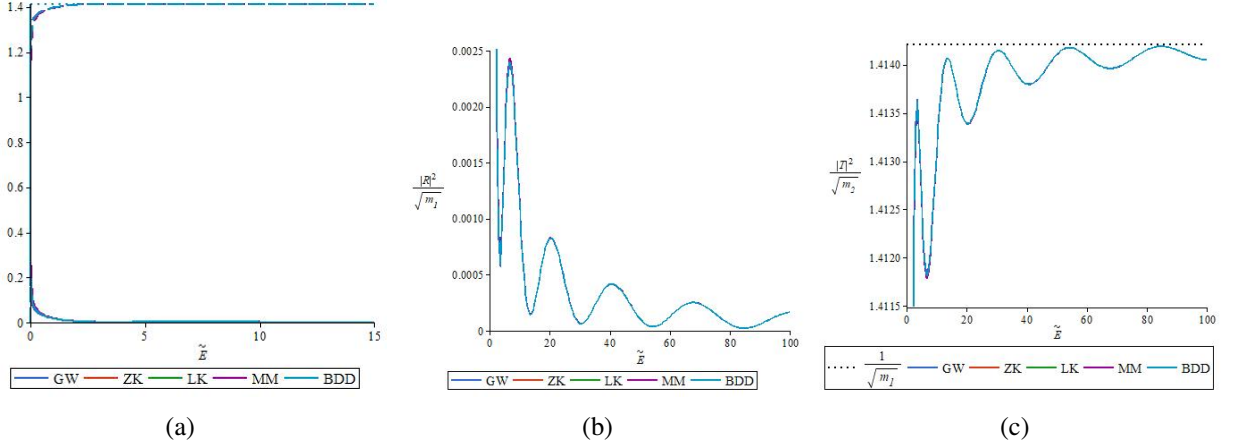


Figure 10: (a) Plot of $|R_{a,b}|^2/\sqrt{m_1}$ and $|T_{a,b}|^2/\sqrt{m_2}$ (solid and dashed lines, respectively). Pointed line corresponds to $|R_{a,b}|^2/\sqrt{m_1} + |T_{a,b}|^2/\sqrt{m_2}$, which equals $1/\sqrt{m_1}$, see eq. (59). (b) and (c) are magnifications of details of Fig. 10(a).

In Fig. 11 we plot the probability densities for some energy levels .

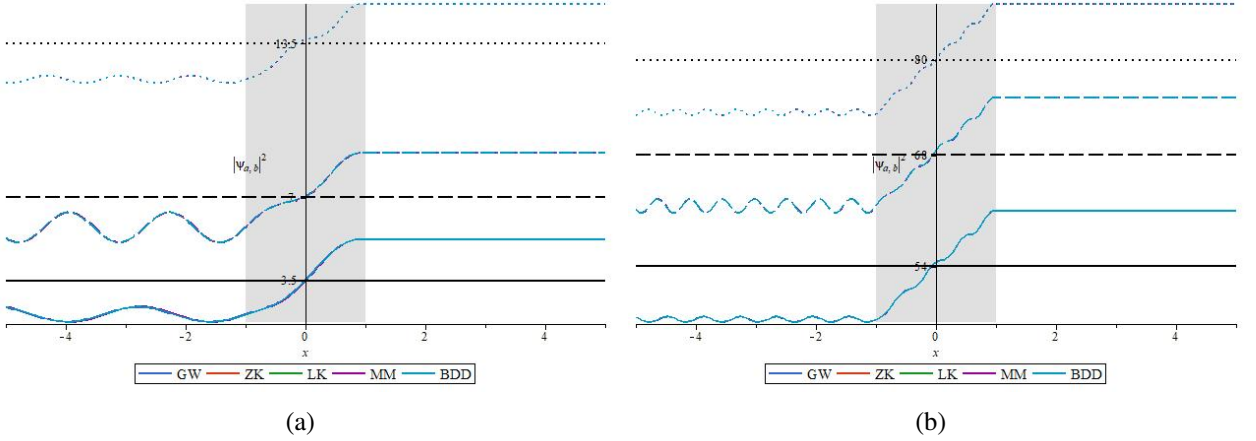


Figure 11: (a) Plots of $|\psi_{a,b}(x)|^2$ for $\tilde{E} = 3.5, 7.0$ and 13.5 (solid, dashed and pointed lines, respectively) and (b) $\tilde{E} = 54, 68$ and 80 (solid, dashed and pointed lines, respectively). The shaded zone is the intermediate region IR where the mass varies with position. The amplitudes are chosen for the sake of visualization and the graphics have been moved up vertically to distinguish energy levels..

5 Final discussion

According to the canonical commutation rules of quantum mechanics, when a position-dependent mass is considered the quantum particle's Hamiltonian can be built in a variety of forms. This would inevitably result in very different energy spectra and particle eigenstates. In this paper we have focused on the study of a purely kinetic Hamiltonian so as to compare the effects of considering

several arrangements of ordering and mass profiles put on an equal footing. For this, we have performed the systematic calculation of the energy eigenvalues and eigenfunctions of Hamiltonians resulting from five different orderings and five distinct spatially depending masses. We have obtained a fully new and large variety of eigenstates arising as a consequence of the different ordering/mass arrangements. Among them, Gauss hypergeometric and Bessel functions related to hyperbolic, exponential or rational functions have been found – see eqs. (17), (31), (43) and (50). In Table 4 we summarize the type of energy spectra of the whole diversity of arrangements. In this table we can see that the reciprocal quadratic mass is the only profile presenting just continuous spectra for every ordering, all with a minimal eigenvalue. For this profile, the only ordering to have an energy gap between the minimum and the continuous band is ZK. The soliton-like, reciprocal biquadratic and exponential profiles admit only discrete spectra and some orderings do not have any allowed physical solutions (GW, ZK and LK for soliton-like, GW and LK for reciprocal biquadratic and only GW for exponential). The parabolic mass is the one profile with less solutions for the whole set of orderings.

Among the different orderings, GW is the only not having physically allowed solutions for any profile but the reciprocal quadratic. MM and BDD, on the other hand, have a full spectrum with a ground state for every mass profile. In the case of discrete spectra, the ZK energy levels are always lower than MM's which in turn are just below those of the BDD ordering (similar comparisons between energy spectra can be found in [67]).

Depending on the arrangement, we have obtained a variety of effective potentials from the pure kinetic PDM Hamiltonian. In Subsections 3.1 and 3.3 we have found even bottomless barriers with discrete spectral solutions associated (e.g. ZK and LK orderings with soliton-like mass). Some authors have addressed the subject of bottomless potentials and provided ways of dealing with these results [68–75]. If we assume that free PDM particles mimic constant mass particles in a solid, we can think of these bottomless barriers as those appearing between the infinite potential wells of nuclei or ions in a crystal. This is a very well-known problem of solid-state physics [76].

We have also verified that some ordering/mass arrangements are discarded for not showing any acceptable solution (neither bound nor scattering eigenstate); this could work as a selection criterion in the search of valid Hamiltonians for a given physical system. Interestingly, MM keeps the potential trivial even in z space; it suggests that the map would be closer to the original. However the solutions are far from trivial.

In Section 4 we applied the approach to the context of a one-dimensional double-heterostructure. We considered no external potential but a PDM of parabolic type in the joining region of two different ordinary constant mass values m_1 and m_2 . We found similarities with the case of ordinary quantum mechanics with transitions among constant potentials (e.g. finite potential-well) where bound states and scattering states can be found depending on the particle energy values. We analytically computed the energy eigenstates as well as reflection and transmission coefficients. For the chosen parameters,

the different orderings showed very similar results as can be seen in Fig.10 and Fig.11. Reflection and transmission coefficients present oscillatory behaviour, respectively decreasing with energy and rapidly convergent to zero, in the first case, or growing and rapidly convergent to $\sqrt{m_2/m_1}$ in the second.

Our results signal that once the spectrum of a given material is experimentally available one could choose the better arrangement among the collection just examined to model the specific material or heterostructure. Indeed, although the external potential is zero, PDM eigenfunctions are not actual free states but a sort of effective waves in a solid sample. This is precisely the origin of the position dependent mass. These states can be more free or more bounded depending on the specific effective mass and operator ordering chosen. Discrete energy eigenstates would represent effective bound electronic states in a crystal, while continuous eigenstates would represent in-solid conduction carriers. Our study is expected to be useful for applications in solid-state structures with the addition of an external potential term.

Table 4: Table of the energy spectra and $\omega_{a,b}$ parameters for each ordering and mass profile (acronyms in parentheses next to the numerical values of $\omega_{a,b}$ denote the shapes of the effective potentials – EP: (IB) for infinite barriers, (FB) for finite barriers, (BB) for bottomless barriers, (IW) for infinite wells, (FW) for finite wells and (BW) for bottomless wells).

Ordering	soliton-like		Reciprocal biquadratic		Reciprocal quadratic		Exponential		Parabolic	
	$\omega_{a,b}$	Energy spectrum (EP)	$\omega_{a,b}$	Energy spectrum (EP)	$\omega_{a,b}$	Energy spectrum (EP)	$\omega_{a,b}$	Energy spectrum (EP)	$\omega_{a,b}$	Energy spectrum (EP)
BDD	$\frac{3}{4}$	Discrete, with minimum; (IW)	2	Discrete, with minimum; (IW)	$\frac{1}{4}$	Continuous, with minimum; (FB)	$\frac{3}{4}$	Discrete, with minimum; (IW)	$\frac{5}{16}$	Depends on $V(x)$ and $M(x)$ outside $ x < \ell$; (IB)
GW	$-\frac{5}{4}$	No spectrum; (BB)	-4	No spectrum; (BB)	$\frac{1}{4}$	Continuous, with minimum; (FB)	$-\frac{5}{4}$	No spectrum; (BB)	$-\frac{7}{16}$	No spectrum; (BW)
ZK	$-\frac{1}{4}$	No spectrum; (BB)	0	Discrete, with minimum; ($cons = -1$)	$-\frac{3}{4}$	Continuous, with minimum and only one bound state; (FW)	$-\frac{1}{4}$	Discrete, with minimum; (BB)	$-\frac{3}{16}$	No spectrum; (BW)
LK	$-\frac{1}{4}$	No spectrum; (BB)	-1	No spectrum; (BB)	$\frac{1}{4}$	Continuous, with minimum; (FB)	$-\frac{1}{4}$	Discrete, with minimum; (BB)	$-\frac{1}{16}$	No spectrum; (BW)
MM	0	Discrete, with minimum; ($cons = 0$)	0	Discrete, with minimum; ($cons = 0$)	0	Continuous, with minimum; ($cons = 0$)	0	Discrete, with minimum; ($cons = 0$)	0	Only $\tilde{E} = 0$ is possible; still, it depends on $V(x)$ and $M(x)$ outside $ x < \ell$; ($cons = 0$)

Acknowledgement

The authors would like to thank Fundo Nacional de Desenvolvimento da Educação do Ministério da Educação (FNDE) for a PET fellowship.

References

- [1] G. H. Wannier, “The structure of electronic excitation levels in insulating crystals,” *Phys. Rev.*, vol. 52, no. 3, p. 191, 1937.
- [2] J. C. Slater, “Electrons in perturbed periodic lattices,” *Phys. Rev.*, vol. 76, no. 11, p. 1592, 1949.
- [3] J. M. Luttinger and W. Kohn, “Motion of electrons and holes in perturbed periodic fields,” *Phys. Rev.*, vol. 97, no. 4, p. 869, 1955.
- [4] D. J. BenDaniel and C. B. Duke, “Space-charge effects on electron tunneling,” *Phys. Rev.*, vol. 152, no. 2, p. 683, 1966.
- [5] T. Gora and F. Williams, “Theory of electronic states and transport in graded mixed semiconductors,” *Phys. Rev.*, vol. 177, no. 3, p. 1179, 1969.
- [6] J. R. Shewell, “On the formation of quantum-mechanical operators,” *Am. J. Phys.*, vol. 27, no. 1, pp. 16–21, 1959.
- [7] O. von Roos, “Position-dependent effective masses in semiconductor theory,” *Phys. Rev. B*, vol. 27, no. 12, p. 7547, 1983.
- [8] J. Thomsen, G. T. Einevoll, and P. C. Hemmer, “Operator ordering in effective-mass theory,” *Phys. Rev. B*, vol. 39, no. 17, p. 12783, 1989.
- [9] J.-M. Lévy-Leblond, “Position-dependent effective mass and Galilean invariance,” *Phys. Rev. A*, vol. 52, no. 3, p. 1845, 1995.
- [10] L. Chetouani, L. Dekar, and T. F. Hammann, “Green’s functions via path integrals for systems with position-dependent masses,” *Phys. Rev. A*, vol. 52, no. 1, p. 82, 1995.
- [11] M. S. Cunha and H. R. Christiansen, “Analytic results in the position-dependent mass Schrödinger problem,” *Commun. Theor. Phys.*, vol. 60, no. 6, p. 642, 2013.
- [12] H. R. Christiansen and M. S. Cunha, “Solutions to position-dependent mass quantum mechanics for a new class of hyperbolic potentials,” *J. Math. Phys.*, vol. 54, no. 12, p. 122108, 2013.

- [13] H. R. Christiansen and M. S. Cunha, “Energy eigenfunctions for position-dependent mass particles in a new class of molecular Hamiltonians,” *J. Math. Phys.*, vol. 55, no. 9, p. 092102, 2014.
- [14] B. G. da Costa, I. S. Gomez, and M. Portesi, “ κ -Deformed quantum and classical mechanics for a system with position-dependent effective mass,” *J. Math. Phys.*, vol. 61, no. 8, p. 082105, 2020.
- [15] C.-L. Ho and P. Roy, “Generalized Dirac oscillators with position-dependent mass,” *EPL-Europhys. Lett.*, vol. 124, no. 6, p. 60003, 2019.
- [16] A. G. M. Schmidt and A. L. de Jesus, “Mapping between charge-monopole and position-dependent mass systems,” *J. Math. Phys.*, vol. 59, no. 10, p. 102101, 2018.
- [17] G. Bastard, J. K. Furdyna, and J. Mycielski, “Landau levels and cyclotron resonance in graded mixed semiconductors,” *Phys. Rev. B*, vol. 12, no. 10, p. 4356, 1975.
- [18] P. Harrison and A. Valavanis, *Quantum Wells, Wires and Dots – Theoretical and Computational Physics of Semiconductor Nanostructures*. New York: John Wiley & Sons, 4th ed., 2016.
- [19] L. Serra and E. Lipparini, “Spin response of unpolarized quantum dots,” *EPL-Europhys. Lett.*, vol. 40, no. 6, p. 667, 1997.
- [20] M. G. Burt, “The justification for applying the effective-mass approximation to microstructures,” *J. Phys.-Condens. Mat.*, vol. 4, no. 32, p. 6651, 1992.
- [21] A. D. Alhaidari, “Solutions of the nonrelativistic wave equation with position-dependent effective mass,” *Phys. Rev. A*, vol. 66, no. 4, p. 042116, 2002.
- [22] A. D. Alhaidari, “Nonrelativistic Green’s function for systems with position-dependent mass,” *Int. J. Theor. Phys.*, vol. 42, no. 12, pp. 2999–3009, 2003.
- [23] J. Yu and S.-H. Dong, “Exactly solvable potentials for the Schrödinger equation with spatially dependent mass,” *Phys. Lett. A*, vol. 325, no. 3-4, pp. 194–198, 2004.
- [24] S.-H. Dong and M. Lozada-Cassou, “Exact solutions of the Schrödinger equation with the position-dependent mass for a hard-core potential,” *Phys. Lett. A*, vol. 337, no. 4-6, pp. 313–320, 2005.
- [25] O. Mustafa and S. H. Mazharimousavi, “Ordering ambiguity revisited via position dependent mass pseudo-momentum operators,” *Int. J. Theor. Phys.*, vol. 46, no. 7, pp. 1786–1796, 2007.

- [26] J. R. F. Lima, M. Vieira, C. Furtado, F. Moraes, and C. Filgueiras, “Yet another position-dependent mass quantum model,” *J. Math. Phys.*, vol. 53, no. 7, p. 072101, 2012.
- [27] R. A. El-Nabulsi, “A generalized self-consistent approach to study position-dependent mass in semiconductors organic heterostructures and crystalline impure materials,” *Phys. E: Low Dim. Syst. Nanostruct.*, vol. 124, p. 114295, 2020.
- [28] R. A. El-Nabulsi, “A new approach to schrodinger equation with position-dependent mass and its implications in quantum dots and semiconductors,” *J. Phys. Chem. Sol.*, vol. 140, p. 109384, 2020.
- [29] M. Barranco, M. Pi, S. M. Gatica, E. S. Hernández, and J. Navarro, “Structure and energetics of mixed ^4He - ^3He drops,” *Phys. Rev. B*, vol. 56, no. 14, p. 8997, 1997.
- [30] M. R. Geller and W. Kohn, “Quantum mechanics of electrons in crystals with graded composition,” *Phys. Rev. Lett.*, vol. 70, no. 20, p. 3103, 1993.
- [31] F. A. de Saavedra, J. Boronat, A. Polls, and A. Fabrocini, “Effective mass of one ^4He atom in liquid ^3He ,” *Phys. Rev. B*, vol. 50, no. 6, p. 4248, 1994.
- [32] M. Willatzen and B. Lassen, “The Ben Daniel–Duke model in general nanowire structures,” *J. Phys.-Condens. Mat.*, vol. 19, no. 13, p. 136217, 2007.
- [33] A. J. Peter and K. Navaneethakrishnan, “Quantum dynamics in low-dimensional systems with position-dependent mass and product-like fractal geometry,” *Phys. E: Low Dim. Syst. Nanostruct.*, vol. 40, pp. 2747–2751, 2008.
- [34] R. A. El-Nabulsi, “Dynamics of position-dependent mass particle in crystal lattices microstructures,” *Phys. E: Low Dim. Syst. Nanostruct.*, vol. 127, p. 114525, 2020.
- [35] H. R. Christiansen and R. Lima, “Three-dimensional bound states of quantum heterostructures with cylindrical symmetry and position-dependent mass carriers,” <http://dx.doi.org/10.2139/ssrn.4140065>, 2023.
- [36] G. Bastard, “Superlattice band structure in the envelope-function approximation,” *Phys. Rev. B*, vol. 24, no. 10, p. 5693, 1981.
- [37] Q.-G. Zhu and H. Kroemer, “Interface connection rules for effective-mass wave functions at an abrupt heterojunction between two different semiconductors,” *Phys. Rev. B*, vol. 27, no. 6, p. 3519, 1983.

- [38] G. Bastard, *Wave Mechanics Applied to Semiconductor Heterostructures*. Les Editions de Physique, 1988.
- [39] I. Galbraith and G. Duggan, “Envelope-function matching conditions for GaAs/(Al,Ga)As heterojunctions,” *Phys. Rev. B*, vol. 38, no. 14, p. 10057, 1988.
- [40] S. Y. Ren and Y.-C. Chang, “Surface states/modes in one-dimensional semi-infinite crystals,” *Ann. Phys.*, vol. 325, no. 5, pp. 937–947, 2010.
- [41] C. Cohen-Tannoudji, B. Diu, and F. Laloë, *Quantum Mechanics*, vol. 1. John Wiley & Sons, 1977.
- [42] L. Dekar, L. Chetouani, and T. F. Hammann, “An exactly soluble Schrödinger equation with smooth position-dependent mass,” *J. Math. Phys.*, vol. 39, no. 5, pp. 2551–2563, 1998.
- [43] L. Dekar, L. Chetouani, and T. F. Hammann, “Wave function for smooth potential and mass step,” *Phys. Rev. A*, vol. 59, no. 1, p. 107, 1999.
- [44] A. R. Plastino, A. Rigo, M. Casas, F. Garcias, and A. Plastino, “Supersymmetric approach to quantum systems with position-dependent effective mass,” *Phys. Rev. A*, vol. 60, no. 6, p. 4318, 1999.
- [45] B. Gönül, B. Gönül, D. Tutcu, and O. Özer, “Supersymmetric approach to exactly solvable systems with position-dependent effective masses,” *Mod. Phys. Lett. A*, vol. 17, no. 31, pp. 2057–2066, 2002.
- [46] S. Karthiga, V. C. Ruby, and M. Senthilvelan, “An inclusive SUSY approach to position dependent mass systems,” *Phys. Lett. A*, vol. 382, no. 25, pp. 1645–1650, 2018.
- [47] B. Roy and P. Roy, “A Lie algebraic approach to effective mass Schrödinger equations,” *J. Phys. A-Math. Gen.*, vol. 35, no. 17, p. 3961, 2002.
- [48] J.-P. Gazeau, V. Hussin, J. Moran, and K. Zelaya, “Quantum and semiclassical aspects of confined systems of variable mass,” *Journal of Physics A: Mathematical and General*, vol. 53, p. 505306, 2020.
- [49] J.-P. Gazeau, V. Hussin, J. Moran, and K. Zelaya, “Two-mode squeezed state quantisation and semiclassical portraits,” *Annals of Physics*, vol. 441, p. 168888, 2020.
- [50] H. Rajbongshi, “Exact analytic solution of position-dependent mass Schrödinger equation,” *Indian J. Phys.*, vol. 92, no. 3, pp. 357–367, 2018.

- [51] L. Jiang, L.-Z. Yi, and C.-S. Jia, “Exact solutions of the Schrödinger equation with position-dependent mass for some Hermitian and non-Hermitian potentials,” *Phys. Lett. A*, vol. 345, no. 4-6, pp. 279–286, 2005.
- [52] O. Mustafa and S. H. Mazharimousavi, “Non-Hermitian d -dimensional Hamiltonians with position-dependent mass and their η -pseudo-Hermiticity generators,” *Czech.J. Phys.*, vol. 56, no. 9, pp. 967–975, 2006.
- [53] C. M. Bender, “ \mathcal{PT} -symmetric quantum theory,” in *Journal of Physics: Conference Series*, vol. 631, p. 012002, IOP Publishing, 2015.
- [54] R. El-Ganainy, M. Khajavikhan, D. N. Christodoulides, and S. K. Ozdemir, “The dawn of non-hermitian optics,” *Communication Physics*, vol. 2, p. 37, 2019.
- [55] T. L. Li and K. J. Kuhn, “Band-offset ratio dependence on the effective-mass Hamiltonian based on a modified profile of the GaAs-Al_xGa_{1-x}As quantum well,” *Phys. Rev. B*, vol. 47, no. 19, p. 12760, 1993.
- [56] R. A. Morrow and K. R. Brownstein, “Model effective-mass Hamiltonians for abrupt heterojunctions and the associated wave-function-matching conditions,” *Phys. Rev. B*, vol. 30, no. 2, p. 678, 1984.
- [57] P. Csavinszky and A. M. Elabsy, “A numerical investigation of model effective-mass Hamiltonians and the associated wavefunction-matching conditions for abrupt heterojunctions,” *Semicond. Sci. Tech.*, vol. 3, no. 10, p. 1010, 1988.
- [58] A. de Souza Dutra and C. A. S. Almeida, “Exact solvability of potentials with spatially dependent effective masses,” *Phys. Lett. A*, vol. 275, no. 1-2, pp. 25–30, 2000.
- [59] W. N. Bailey, *Generalized hypergeometric series*. No. 32 in Cambridge Tracts in Mathematics, Hafner Publishing Co Ltd, New ed., 1973.
- [60] P. M. Mathews and M. Lakshmanan, “A quantum-mechanically solvable nonpolynomial lagrangian with velocity-dependent interaction,” *Il Nuovo Cimento A (1965-1970)*, vol. 26, no. 3, pp. 299–316, 1975.
- [61] P. M. Mathews and M. Lakshmanan, “On a unique nonlinear oscillator,” *Quarterly of Applied Mathematics*, vol. 32, no. 2, pp. 215–218, 1974.
- [62] S. C. y Cruz, J. Negro, and L. M. Nieto, “Classical and quantum position-dependent mass harmonic oscillators,” *Phys. Lett. A*, vol. 369, no. 5-6, pp. 400–406, 2007.

- [63] S. Karthiga, V. Chithiika Ruby, M. Senthilvelan, and M. Lakshmanan, “Quantum solvability of a general ordered position dependent mass system: Mathews-Lakshmanan oscillator,” *Journal of Mathematical Physics*, vol. 58, no. 10, p. 102110, 2017.
- [64] B. Midya, B. Roy, and T. Tanaka, “Effect of position-dependent mass on dynamical breaking of type B and type X_2 \mathcal{N} -fold supersymmetry,” *Journal of Physics A: Mathematical and Theoretical*, vol. 45, no. 20, p. 205303, 2012.
- [65] J. P. G. Nascimento and I. Guedes, “Osciladores clássicos com massa dependente da posição,” *Rev. Bras. Ensino Fis.*, vol. 36, no. 4, pp. 01–06, 2014.
- [66] A. G. M. Schmidt, “Wave-packet revival for the Schrödinger equation with position-dependent mass,” *Phys. Lett. A*, vol. 353, no. 6, pp. 459–462, 2006.
- [67] D. Kulikov, “Comparison theorems for the position-dependent mass Schrödinger equation,” *International Scholarly Research Notices*, vol. 2012, p. 461452, 2012.
- [68] T. Vachaspati, “Bound states in bottomless potentials,” *Physical Review A*, vol. 66, no. 1, p. 014104, 2002.
- [69] A. Sous and M. El-Kawni, “General eigenvalue problems with unbounded potential from below,” *International Journal of Modern Physics A*, vol. 24, no. 22, pp. 4169–4176, 2009.
- [70] A. Demić, V. Milanović, J. Radovanović, and M. Musić, “WKB method for potentials unbounded from below,” *Modern Physics Letters B*, vol. 30, no. 03, p. 1650003, 2016.
- [71] Z. Ahmed, D. Ghosh, S. Kumar, and N. Turumella, “Solvable models of an open well and a bottomless barrier: one-dimensional exponential potentials,” *European Journal of Physics*, vol. 39, no. 2, p. 025404, 2018.
- [72] M. Hu, K. Guo, Q. Yu, and Z. Zhang, “Third-harmonic generation investigated by a short-range bottomless exponential potential well,” *Superlattices and Microstructures*, vol. 122, pp. 538–547, 2018.
- [73] Z. Ahmed, S. Kumar, D. Ghosh, and T. Goswami, “Solvable model of bound states in the continuum (BIC) in one dimension,” *Physica Scripta*, vol. 94, no. 10, p. 105214, 2019.
- [74] H.-T. Cho and C.-L. Ho, “A novel quasi-exactly solvable model with total transmission modes,” *Journal of Physics A: Mathematical and Theoretical*, vol. 41, no. 17, p. 172002, 2008.
- [75] H.-T. Cho and C.-L. Ho, “Self-adjoint extensions of the hamiltonian operator with symmetric potentials which are unbounded from below,” *Journal of Physics A: Mathematical and Theoretical*, vol. 41, no. 25, p. 255308, 2008.

[76] C. Cohen-Tannoudji, B. Diu, and F. Laloë, *Quantum Mechanics*, vol. 2. John Wiley and Sons, 1978.